

COUPLING OF RADIAL MULTIPLE SLE WITH GAUSSIAN FREE FIELD, AND THE HYDRODYNAMIC LIMIT

MAKOTO KATORI, SHINJI KOSHIDA, CHIZURU SOUKEJIMA, AND RAIAN SUZUKI

ABSTRACT. Schramm–Loewner evolution (SLE) has been one of the central topics in the probabilistic study of two-dimensional critical systems. It is a random curve in two dimensions to which a cluster interface in a critical lattice system is supposed, or has been proved, to converge. The most archetypical setting for SLE is called chordal, where a random curve evolves in a simply-connected domain from a boundary point to another, whereas in its variant called radial, a random curve evolves from a boundary point to a distinguished interior point. Multiple SLE is a variant to another direction; it deals with multiple random curves, and it is a natural direction as there are certainly multiple cluster interfaces found in critical lattice systems. In this paper, we study multiple SLE in the radial setting, namely, radial multiple SLE.

We report two main results. One is regarding coupling between radial multiple SLE and Gaussian free field (GFF). Coupling between SLE and GFF has been extensively studied in the chordal setting, and serves as a foundation for many recent developments. We show that coupling between radial multiple SLE and GFF occurs if and only if the radial multiple SLE is driven by the circular Dyson Brownian motions.

The circular Dyson Brownian motions is a typical example of stochastic log-gas. This fact motivates us to study the hydrodynamic limit of the corresponding radial multiple SLE, which refers to the dynamical law of large numbers, when the number of curves tends to infinity. In our other main result, we provide explicit description of the hydrodynamic limit.

CONTENTS

1. Introduction	2
1.1. Background	2
1.2. Radial SLE	4
1.3. Summary of the results	5
1.4. Discussion	10
Organization of the paper	12
Acknowledgments	12
2. Gaussian free field	13
2.1. Definition	13
2.2. Domain Markov property	15
3. Coupling	15
3.1. Motivating example: single-curve case	15
3.2. Multiple curve case	19

Date: August 20, 2025.

4.	Hydrodynamic limit	24
4.1.	Hydrodynamic limit of circular Dyson Brownian motions	24
4.2.	Hydrodynamic limit of multiple SLE and factorization	27
4.3.	Solution for the Loewner chain	28
4.4.	Analysis of the map Ω_t	30
4.5.	Boundary curve of the SLE hull	32
4.6.	Edge asymptotics	34
	References	36

1. INTRODUCTION

1.1. Background.

Schramm–Loewner evolution. Schramm–Loewner evolution (SLE) [Sch00] is a random continuous curve in a two-dimensional domain that is conformally invariant and satisfies the domain Markov property. In the most studied *chordal* case, the curve evolves between two boundary points. Due to the conformal invariance, we may assume that the domain is the complex upper-half plane $\mathbb{H} = \{z \in \mathbb{C} | \text{Im} z > 0\}$, and that the curve evolves from 0 to ∞ . Thanks to the Loewner theory from complex analysis, such a curve is governed by the chordal Loewner equation

$$(1.1) \quad \begin{aligned} \frac{d}{dt}g_t(z) &= \frac{2}{g_t(z) - X_t}, \quad t \geq 0, \\ g_0(z) &= z \in \mathbb{H}, \end{aligned}$$

where $(X_t : t \geq 0)$ is a continuous stochastic process on \mathbb{R} called the driving process. The solution $(g_t : t \geq 0)$ is called a Loewner chain and, at each $t \geq 0$,

$$g_t : \mathbb{H}_t \rightarrow \mathbb{H}$$

is conformal¹, where $\mathbb{H}_t \subset \mathbb{H}$ is the set of $z \in \mathbb{H}$ for which (1.1) has a solution until $t \geq 0$. The original curve, which is denoted by $\eta : [0, \infty) \rightarrow \overline{\mathbb{H}}$, is recovered from the Loewner chain as

$$\eta_t = \lim_{\epsilon \downarrow 0} g_t^{-1}(X_t + i\epsilon), \quad t \geq 0.$$

where $i = \sqrt{-1}$.

Remarkably, the driving process must be $X_t = \sqrt{\kappa}B_t$, $t \geq 0$ where $(B_t : t \geq 0)$ is a standard Brownian motion and $\kappa \geq 0$ when the law of η is conformally invariant and satisfies the domain Markov property [Sch00]. With this choice of a driving process, the curve η is indeed continuous [RS05]. In other words, there is a unique SLE for each $\kappa \geq 0$. More detailed and thorough account of SLE can be found in [Law05, Kat15, Kem17].

¹In this paper, we call a bijective conformal map simply a conformal map.

Critical lattice systems and conformal field theory. SLE was introduced in the study of critical lattice models in two dimensions as a candidate for a scaling limit of a domain interface. In fact, the two characterizing properties of SLE, conformal invariance and domain Markov property, are naturally expected for a scaling limit of a domain interface. There are by now various critical lattice models whose domain interface is proved to converge to an SLE [Smi01, LSW04, SS05, SS09, CDCH⁺14].

A critical lattice system in two dimensions is also conjectured to give a conformal field theory (CFT) [BPZ84a, BPZ84b] in a scaling limit. Therefore, one might expect an interrelation between SLE and CFT as both capture some properties of scaling limits of critical lattice systems. Such an interrelation was studied right after the introduction of SLE and dubbed the SLE/CFT-correspondence [BB02, BB03, BB04b, FW03, FK04, KS07, Kyt07, Dub15b, Dub15a]. It would be more appropriate to call it a *coupling* rather than *correspondence*, though, because of the reason explained next.

Gaussian free field. While the above mentioned studies of the SLE/CFT-correspondence were more or less based on the representation theory of the Virasoro algebra as a formulation of CFT, Schramm and Sheffield [SS13] found a purely probabilistic instance of the SLE/CFT-correspondence using Gaussian free field (GFF), which is a probabilistic avatar of the CFT of massless free bosons. In their work, the SLE/CFT-correspondence was realized as a coupling between SLE and GFF. Coupling between SLE and GFF was studied further [Dub09] and serves as a foundation of the Liouville quantum gravity [DMS14, She16, AHS23a, AHSY23], imaginary geometry [MS16a, MS16b, MS16c, MS17], and various other developments [KM13, Kos21, KK20, KK21a, AHS23b, BKT23, ABK24, AB24, ACSW24, AHS24].

Multiple SLE. From the original motivation for SLE, it is natural to extend it to deal with multiple random curves in a two-dimensional domain because there could be certainly found multiple domain interfaces in a critical lattice model. Such an extension is called multiple SLE. Similarly to the single curve case, convergence to multiple SLE has been proven for various critical lattice models [Izy15, Izy17, BPW21, Kar19, PW19, Kar20, Izy22, PW23b].

A global definition of multiple SLE [KL07, BPW21] is concise and conceptual, but its local model based on the Loewner theory is also useful for some purposes. There are actually two local models of multiple SLE; one is a commuting family of Loewner chains [Dub07] and the other is a single Loewner chain driven by a multi-particle stochastic process [BBK05, Gra07, Sch12, RS17].

The two approaches are equivalent at least as long as the curves are apart from each other, but the latter is closer to our point of view. For $N \geq 1$, a multiple SLE with N -curves is the Loewner chain that solves the multiple Loewner equation

$$(1.2) \quad \begin{aligned} \frac{d}{dt}g_t(z) &= \sum_{i=1}^N \frac{2}{g_t(z) - X_t^{(i)}}, \quad t \geq 0, \\ g_0(z) &= z \in \mathbb{H}, \end{aligned}$$

where $(X_t^{(i)} : t \geq 0)$, $i = 1, \dots, N$ are continuous stochastic processes whose laws are determined by what is called a partition function. See [BBK05] for the stochastic differential equations for the driving processes in terms of a partition function. Equation (1.2) is obviously an extension of (1.1), and similarly, we may find $\mathbb{H}_t \subset \mathbb{H}$ at each $t \geq 0$ so that

$$g_t : \mathbb{H}_t \rightarrow \mathbb{H}$$

is conformal. Furthermore, N curves $\eta^{(i)} : [0, \infty) \rightarrow \overline{\mathbb{H}}$, $i = 1, \dots, N$ are found as

$$\eta_t^{(i)} = \lim_{\epsilon \downarrow 0} g_t^{-1}(X_t^{(i)} + i\epsilon), \quad t \geq 0, \quad i = 1, \dots, N.$$

Within the framework of multiple SLE, we can at best say that a partition function must satisfy the set of Belavin–Polyakov–Zamolodchikov equations for some consistency [Dub07]. However, there is no intrinsic principle that allows us to fix a partition function uniquely. In other words, the laws of the driving processes $(X_t^{(i)} : t \geq 0)$, $i = 1, \dots, N$ in (1.2) are another input than (1.2) itself.

Dyson Brownian motions. On the other hand, there should be a unique law of multiple curves when we know that they are a scaling limit of domain interfaces of a critical lattice model. In other words, one should be able to fix a partition function, or equivalently, driving processes by assuming coupling with a specific CFT under specific boundary conditions. In the previous work by the first two authors [KK21b], we studied coupling between multiple SLE and GFF. In upshot, coupling is possible if and only if the driving processes are the Dyson Brownian motions [Dys62] with the parameter determined by the boundary conditions of the GFF. The Dyson Brownian motions originally arose as a dynamical version of the Gaussian ensemble of random matrices and were extended as stochastic particle systems with logarithmic interaction potential, as known as stochastic log-gases. Therefore, our result is to intertwine stochastic log-gases including dynamical random matrix theory and multiple SLE through GFF.

Hydrodynamic limit. One of the typical problems regarding a stochastic particle system is its *hydrodynamic limit*. This is a dynamical analogue of the law of large numbers. In the random matrix terminology, we can think of it as a large N -limit, or a dynamical analogue of Wigner’s semi-circular law. In the case of Dyson Brownian motions, the hydrodynamic limit is well-established [AGZ10]. The hydrodynamic limit of the corresponding multiple SLE was studied in [dMS16, dMHS18] and exactly solved by Hotta and the first author [HK18].

1.2. Radial SLE. All the above results are regarding the chordal setting. A variant of the chordal SLE is the *radial* SLE, where a curve runs between a boundary point and a distinguished interior point.

Due to the conformal invariance, we may pick the unit disk $\mathbb{D} = \{z \in \mathbb{C} \mid |z| < 1\}$ as a domain of interest, and suppose that the curve evolves from 1 to 0. Similarly to the

chordal case, we rely on the Loewner theory to describe the curve. The radial Loewner equation reads

$$(1.3) \quad \begin{aligned} \frac{d}{dt}g_t(z) &= -g_t(z)\frac{g_t(z) + X_t}{g_t(z) - X_t}, \quad t \geq 0, \\ g_0(z) &= z \in \mathbb{D}, \end{aligned}$$

where the driving process $(X_t : t \geq 0)$ is continuous on the unit circle $\mathbb{S} = \{z \in \mathbb{C} \mid |z| = 1\}$. Again, for each $t \geq 0$, we define \mathbb{D}_t as the set of $z \in \mathbb{D}$ such that the solution of (1.3) exists until the time t . Then, $g_t : \mathbb{D}_t \rightarrow \mathbb{D}$ is conformal at each $t \geq 0$. A curve $\eta : [0, \infty) \rightarrow \overline{\mathbb{D}}$ is obtained by

$$\eta_t = \lim_{r \uparrow 1} g_t^{-1}(rX_t), \quad t \geq 0.$$

For the law of the curve to be conformally invariant and satisfy the domain Markov property, the driving process must be $X_t = e^{i\sqrt{\kappa}B_t}$, $t \geq 0$ with $\kappa \geq 0$ and a standard Brownian motion $(B_t : t \geq 0)$.

It is natural to expect that an analogous story as in the previous section exists for the radial setting as well. In fact, the SLE/CFT-correspondence (or coupling) in the radial setting has been studied in [BB04a]. As its probabilistic instance, [IK13] studied the coupling between the radial SLE at $\kappa = 4$ and GFF.

1.3. Summary of the results. In this paper, we explore coupling between radial multiple SLE and GFF, thereby extending the results of both [KK21b] in the chordal setting and [IK13] in the single-curve setting.

Our local model for radial multiple SLE is the following natural extension of (1.3): with $N \geq 1$,

$$(1.4) \quad \begin{aligned} \frac{d}{dt}g_t(z) &= -\sum_{i=1}^N g_t(z)\frac{g_t(z) + X_t^{(i)}}{g_t(z) - X_t^{(i)}}, \quad t \geq 0, \\ g_0(z) &= z \in \mathbb{D}, \end{aligned}$$

driven by continuous driving processes $(X_t^{(i)} : t \geq 0)$, $i = 1, \dots, N$ on \mathbb{S} . The solution is a family of conformal maps $g_t : \mathbb{D}_t \rightarrow \mathbb{D}$, $t \geq 0$, and N curves $\eta^{(i)} : [0, \infty) \rightarrow \overline{\mathbb{D}}$, $i = 1, \dots, N$ are defined by

$$\eta_t^{(i)} := \lim_{r \uparrow 1} g_t^{-1}(rX_t^{(i)}), \quad t \geq 0, \quad i = 1, \dots, N.$$

See Figure 1 for illustration. Note that the curves $\eta^{(i)}$, $i = 1, \dots, N$ might not be continuous because the driving processes are yet unknown. Nevertheless, the domains \mathbb{D}_t , $t \geq 0$ on which the conformal maps g_t , $t \geq 0$ are defined make sense. For completeness, we write $K_t := \mathbb{D} \setminus \mathbb{D}_t$, $t \geq 0$ and call it the SLE hull.

Definition 1.1. We call the solution of (1.4) the *radial multiple SLE* driven by $(X_t^{(i)} : t \geq 0)$, $i = 1, \dots, N$.

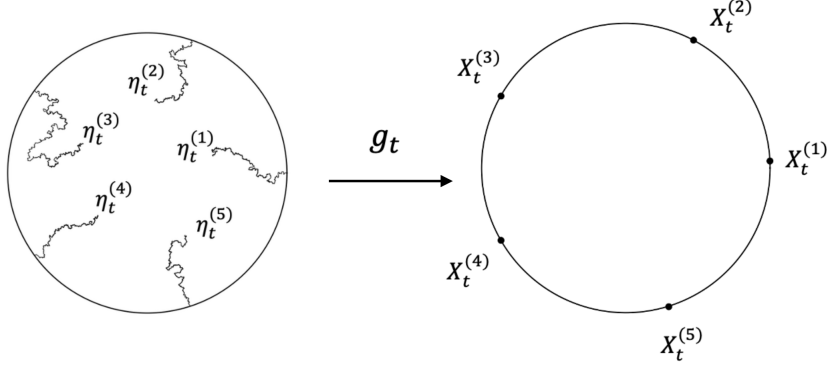


FIGURE 1. A schematic picture of $g_t: \mathbb{D}_t \rightarrow \mathbb{D}$ at time $t > 0$. The tips of SLE curves, $\eta_t^{(i)}$, $i = 1, \dots, N$ are mapped to the points $X_t^{(i)}$, $i = 1, \dots, N$ on \mathbb{S} , respectively.

Similarly to the chordal case, coupling of a radial multiple SLE to GFF provides enough information to fix the driving processes. To state the result, let us first recall the *circular Dyson Brownian motions*.

Definition 1.2. Let $N \geq 1$ and $\beta > 0$. The N -particle *circular β -Dyson Brownian motions* are $(X_t^{(i)} = e^{i\Theta_t^{(i)}} \in \mathbb{S} : t \geq 0)$, $i = 1, \dots, N$ that solve the system of stochastic differential equations (SDEs)

$$(1.5) \quad d\Theta_t^{(i)} = \sqrt{\frac{8}{\beta}} dB_t^{(i)} + 2 \sum_{\substack{j=1 \\ j \neq i}}^N \cot \left(\frac{\Theta_t^{(i)} - \Theta_t^{(j)}}{2} \right) dt, \quad i = 1, \dots, N,$$

where $(B_t^{(i)} : t \geq 0)$, $i = 1, \dots, N$ are mutually independent standard Brownian motions.

Remark 1.3. The system of SDEs (1.5) seems non-standard. In fact, the processes $(X_{\beta t/8}^{(i)} : t \geq 0)$, $i = 1, \dots, N$ after changing the time scale are often referred to as the circular β -Dyson Brownian motions. The reason for the peculiar coefficient $\sqrt{8/\beta}$ is that we will match $8/\beta$ with the SLE parameter κ .

We will provide a definition of the coupling between radial multiple SLE and GFF in Section 3. In our context, a GFF refers to the sum of the zero-boundary GFF and a deterministic harmonic function. Thus, we need to pick a harmonic function to specify a GFF. We will find a family of GFFs parametrized by $\kappa > 0$ so that the following holds. (See Theorem 3.4 for precise statement.)

Theorem 1.4. *The GFF with parameter $\kappa > 0$ is coupled with a radial multiple SLE if and only if the radial multiple SLE is driven by the circular $8/\kappa$ -Dyson Brownian motions.*

The circular Dyson Brownian motions are a natural analogue of the Dyson Brownian motions on the unit circle. The hydrodynamic limit of the circular Dyson Brownian motions is well-known [CL01]. To explain the hydrodynamic limit of the corresponding

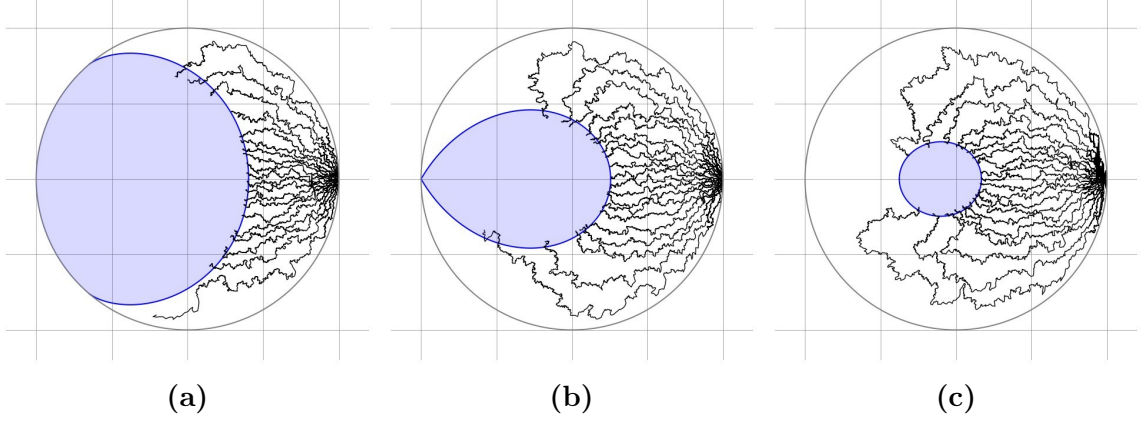


FIGURE 2. Samples of radial SLE curves $\eta_t^{(i)}$, $i = 1, \dots, N$ with $N = 20$, all started from $z = 1$, are drawn by numerical simulation for $\kappa = 8/\beta = 2$ at time (a) $t = 0.5$, (b) $t = t_c = 1$ (critical time), (c) $t = 1.5$, respectively. At each time, as $N \rightarrow \infty$, SLE curves become denser and formulate a subdomain of \mathbb{D} which we call the SLE hull $K_t^{[\infty]}$. The domains of $g_t^{[\infty]}$ given by $\mathbb{D}_t^{[\infty]} = \mathbb{D} \setminus K_t^{[\infty]}$ are shown by the shaded subdomains of \mathbb{D} and the boundary curves of the SLE hulls γ_t are drawn by thick lines for each time. The SLE hull $K_t^{[\infty]}$ changes its topology at t_c from a disk to an annulus

radial multiple SLE, let us first manifest N in our notation. For each $N \geq 1$, we will write $(g_t^{[N]} : t \geq 0)$ for the multiple radial SLE driven by the N -particle circular β -Dyson Brownian motions $(X_t^{(i)} : t \geq 0)$, $i = 1, \dots, N$, with any $\beta > 0$, and $(\mathbb{D}_t^{[N]} : t \geq 0)$ for the corresponding evolution of domain.

Along with the hydrodynamic limit $N \rightarrow \infty$, we assume that the initial conditions for the circular Dyson Brownian motions satisfy

$$(1.6) \quad \frac{1}{N} \sum_{i=1}^N \delta_{X_0^{(i)}}(\cdot) \xrightarrow{\text{weak}} \delta_1(\cdot) \quad \text{as } N \rightarrow \infty.$$

Here, the Dirac (point-mass) measure on \mathbb{S} is defined by

$$\delta_x(A) = \begin{cases} 1, & x \in A, \\ 0, & \text{otherwise,} \end{cases}$$

for $x \in \mathbb{S}$ and Borel measurable $A \subset \mathbb{S}$.

It has been show in [HS21] that, for each $t \geq 0$, the conformal map $g_{t/N}^{[N]}$ converges locally uniformly in distribution as $N \rightarrow \infty$. This is equivalent to that $\mathbb{D}_{t/N}^{[N]}$ converges in the Caratheodory kernel sense. Let us write these limits as $g_t^{[\infty]} = \lim_{N \rightarrow \infty} g_{t/N}^{[N]}$ and $\mathbb{D}_t^{[\infty]} = \lim_{N \rightarrow \infty} \mathbb{D}_{t/N}^{[N]}$, $t \geq 0$, and call them the *hydrodynamic limits of the radial multiple SLE*. We also set $K_t^{[\infty]} := \mathbb{D} \setminus \mathbb{D}_t^{[\infty]}$, $t \geq 0$, which is called the *SLE hull in the hydrodynamic*

limit. Figure 2 shows numerical simulation of the radial SLE curves $\eta_t^{(i)}$, $i = 1, \dots, N$ with $N = 20$ for $\kappa = 8/\beta = 2$ at $t = 0.5, 1.0$, and 1.5 , under the initial condition $X_0^{(i)} = \eta_0^{(i)} = 1$ for all $i = 1, \dots, N$. As N grows, the SLE curves will become denser, and the SLE hull will be eventually a subdomain $K_t^{[\infty]}$ of \mathbb{D} such that $e^{\pm i\varepsilon} \in \overline{K_t^{[\infty]}}$, $0 \leq \varepsilon \ll 1$, but $0 \notin K_t^{[\infty]}$, $0 < t < \infty$. The limit family of conformal maps $(g_t^{[\infty]} : t \geq 0)$ solves a measure-driven Loewner equation [HS21] (see Proposition 4.6) that allows for further analysis. It is worth noting that the hydrodynamic limit does not depend on the parameter β for the circular Dyson Brownian motions.

Here we report exact and explicit description of $g_t^{[\infty]}$ and $\mathbb{D}_t^{[\infty]}$ for $t \geq 0$. Let W_0 be the complex Lambert function used in [HK18] (see Section 4.3 for definition), and put

$$(1.7) \quad \Lambda_t(z) = 4t \frac{z}{(1-z)^2}.$$

Then, the Loewner chain $(g_t^{[\infty]} : t \geq 0)$ admits the following expression.

Theorem 1.5. *At each $t \geq 0$, we have*

$$g_t^{[\infty]}(z) = \left[1 + \frac{2t}{W_0(\Lambda_t(z)e^{-t})} \left(1 - \sqrt{1 + W_0(\Lambda_t(z)e^{-t})/t} \right) \right] e^{2t\sqrt{1+W_0(\Lambda_t(z)e^{-t})/t}}.$$

To present the result for $\mathbb{D}_t^{[\infty]}$, $t \geq 0$, we need a couple of auxiliary functions. First, we define $x_t^{\max} \geq 0$, $t \in [0, \infty)$ and $x_t^{\min} \geq 0$, $t \in [1, \infty)$ by the equations

$$(1.8) \quad \frac{x_t^{\max}}{2} \tanh \frac{x_t^{\max}}{2} = t \quad \text{and} \quad \frac{x_t^{\min}}{2} \coth \frac{x_t^{\min}}{2} = t.$$

It can be readily checked that both are monotonically increasing in t , $x_0^{\max} = x_1^{\min} = 0$, $x_t^{\min} < x_t^{\max}$ for $t \in [1, \infty)$, and $\lim_{t \rightarrow \infty} x_t^{\max} = \lim_{t \rightarrow \infty} x_t^{\min} = +\infty$. Next, we introduce

$$(1.9) \quad \Phi_t(x) := 2 \operatorname{arcsinh} \left[-\sqrt{\frac{te^{-t}}{u(x)}} \exp \left(-i\psi_t(x) - \frac{u(x)}{2} e^{2i\psi_t(x)} \right) \right]$$

with

$$(1.10) \quad u(x) = \frac{x}{\sinh x},$$

$$(1.11) \quad \psi_t(x) = \frac{1}{2} \arccos \left(\frac{x}{2t} \sinh x - \cosh x \right)$$

Then,

$$(1.12) \quad \gamma_t^+ = \begin{cases} \{\gamma_t^+(x) = e^{\Phi_t(x)} \mid x \in [0, x_t^{\max}]\}, & \text{if } 0 < t \leq 1, \\ \{\gamma_t^+(x) = e^{\Phi_t(x)} \mid x \in [x_t^{\min}, x_t^{\max}]\}, & \text{if } t > 1 \end{cases}$$

gives a simple curve in $\overline{\mathbb{D} \cap \mathbb{H}}$ with the endpoints

$$\begin{aligned} \gamma_t^{+\text{out}} &:= \begin{cases} \gamma_t^+(0) = \begin{cases} e^{i\varphi_t^c} \in \mathbb{S} \cap \mathbb{H}, & \text{for } 0 < t < 1, \\ -1, & \text{for } t = 1, \end{cases} \\ \gamma_t^+(x_t^{\min}) \in (-1, 0), & \text{for } 1 < t < \infty, \end{cases} \\ \gamma_t^{+\text{in}} &:= \gamma_t^+(x_t^{\max}) \in (0, 1), \quad \text{for } 0 < t < \infty, \end{aligned}$$

where

$$(1.13) \quad \varphi_t^c = 2 \arcsin(\sqrt{t}e^{(1-t)/2}) = \arccos(1 - 2te^{1-t}).$$

Note that

$$\gamma_t^+ \setminus \{\gamma_t^{+\text{out}}, \gamma_t^{+\text{in}}\} \subset \mathbb{D} \cap \mathbb{H}.$$

Remark 1.6. To find out these endpoints, it is useful to notice that $\psi_t(x)$ admits various expressions. In fact, we have

$$\psi_t(x) = \arcsin\left(\sqrt{1 - \frac{x}{2t} \tanh \frac{x}{2} \cosh \frac{x}{2}}\right), \quad t > 0, \quad x \leq x_t^{\max}$$

that gives $\psi_t(x_t^{\max}) = 0$, $t > 0$ and $\psi_t(0) = \frac{\pi}{2}$, $0 < t \leq 1$. Another formula reads

$$\psi_t(x) = \arccos\left(\sqrt{\frac{2}{2t} \coth \frac{x}{2} - 1 \sinh \frac{x}{2}}\right), \quad t > 1, \quad x \geq x_t^{\min}$$

that gives $\psi_t(x_t^{\min}) = \frac{\pi}{2}$, $t > 1$.

For each $t \geq 0$, let $\gamma_t^- = (\gamma_t^+)^*$ be the complex conjugate of (1.12), and set

$$(1.14) \quad \gamma_t := \gamma_t^+ \cup \gamma_t^-.$$

We also understand $\gamma_0 := \lim_{t \downarrow 0} \gamma_t^+ = \{\lim_{t \downarrow 0} \gamma_t^+(0)\} = \{\lim_{t \downarrow 0} \gamma_t^+(x_t^{\max})\} = \{1\}$. We can see that γ_t for $t > 0$ cuts \mathbb{D} into two connected components. With these preliminaries, we can identify the domains $\mathbb{D}_t^{[\infty]}$, $t \geq 0$ as follows.

Theorem 1.7. *At each $t \geq 0$, $\mathbb{D}_t^{[\infty]}$ is the connected component of $\mathbb{D} \setminus \gamma_t$ that contains 0.*

From the explicit formula for $(\gamma_t : t \geq 0)$, we can see the following. There is a *critical time* $t_c = 1$ such that

- (1) when $0 < t < t_c$, $\gamma_t = (\partial K_t^{[\infty]} \cap \mathbb{D}) \cup \{\gamma_t^{+\text{out}}, (\gamma_t^{+\text{out}})^*\}$,
- (2) when $t = t_c$, $\gamma_{t_c} = (\partial K_{t_c}^{[\infty]} \cap \mathbb{D}) \cup \{\gamma_{t_c}^{+\text{out}} = (\gamma_{t_c}^{+\text{out}})^* = -1\}$,
- (3) when $t > t_c$, $\gamma_t = \partial K_t^{[\infty]} \subset \mathbb{D}$.

In particular, the SLE hull $K_t^{[\infty]}$ changes its topology at time t_c from a disk to an annulus as is also demonstrated in Figure 2. We will often call γ_t with $t \geq 0$ the boundary curve of the SLE hull though it does not necessarily coincide with $\partial K_t^{[\infty]}$.

Remark 1.8. For $0 < t \ll 1$, (1.8) gives $(x_t^{\max})^2/4 \sim t$. We parameterize $x \in [0, 2\sqrt{t}]$ as $x = 2\sqrt{t} \cos \vartheta$, $\vartheta \in [0, \pi/2]$. Equations (1.10) and (1.11) give $u(x) \sim 1$ and $\psi_t(x) \sim$

$\arccos(2\cos^2\vartheta - 1)/2 = \vartheta$, respectively. Hence, the boundary curve of the SLE hull (1.14) with (1.12) is reduced to

$$(1.15) \quad \gamma_t = \left\{ 1 - 2\sqrt{t} \exp\left(-i\vartheta - \frac{1}{2}e^{2i\vartheta}\right) \middle| \vartheta \in [-\pi/2, \pi/2] \right\}.$$

If we map the tangent line to the unit circle \mathbb{S} at $z = 1$ to \mathbb{R} centered at the origin, then the short-term behavior (1.15) is identified with the exact expression of the boundary curve of SLE hull in the hydrodynamic limit starting from δ_0 in \mathbb{H} , which was derived in [HK18] for the chordal multiple SLE. In other words, the present exact solution of the boundary curve of the SLE hull (1.14) with (1.12) can be regarded as a trigonometric-hyperbolic extension of (1.15).

1.4. Discussion.

Relation to other work. The circular Dyson Brownian motions were first proposed as the natural driving processes of radial multiple SLE in [Car03]. More recently, [HL21] also suggested that the radial multiple SLE should be driven by the circular Brownian motions. The starting point of [HL21] is the fact [KL07] that the global multiple SLE in the chordal setting is obtained by reweighting independent SLEs using Brownian loop measures. Their requirement on radial multiple SLE is that it is realized as a certain limit of this construction.

Both [Car03] and [HL21] assume that, with radial multiple SLE, each curve is absolutely continuous with respect to a single radial SLE, which is of course reasonable. It seems to be the case that the driving processes need to be the circular Dyson Brownian motions when all curves must go to the origin. In contrast, in the present work, we do not assume such absolute continuity, not even that the radial multiple SLE actually generates continuous curves. Nonetheless, we can fix the driving processes by assuming coupling with GFF.

β -ensemble on the boundary. The other result of [Car03] is that, in a reasonable situation, the radial multiple SLE evolves from random boundary points obeying the circular β -ensemble, the invariant measure of the circular β -Dyson Brownian motions. Though, in the present work, the radial multiple SLE evolves from fixed boundary points, it is interesting to see if GFF realizes a situation where the curves evolve from random boundary points.

In this direction, we find the recent [Liu25] interesting. The result therein is that, a certain chordal multiple SLE curves coupled with GFF hit random boundary points in an interval that obeys the β -Jacobi ensemble. If a similar approach is possible in the radial case, it could give an answer to the above question.

Origin of (circular) Dyson Brownian motions. Either on the real axis or the unit circle, the (circular) Dyson Brownian motions have a long history. On the real axis, the Dyson Brownian motions for $\beta = 1, 2, 4$ are eigenvalue processes of dynamical random matrices [Dys62]. The circular Dyson Brownian motions for $\beta = 2$ also appeared as an eigenvalue process in the same paper. At the level of SDEs, it seems natural to extend the

parameter to $\beta > 0$ as it is interpreted as the strength of interaction. In fact, this generalization has led to numerous achievements in the field of stochastic log-gases [CL97, CL01].

However, once we step back and ask why this generalization to $\beta > 0$ is a right direction, we find the origins of general β -Dyson Brownian motions quite subtle. One natural expectation would be that they also appear as eigenvalue processes of some dynamical random matrices. Potentially, this sounds promising since the static β -ensemble can be realized as an eigenvalue ensemble of a tridiagonal random matrix [DE02]. However, there turns out to be a discrepancy between one dynamical model of this tridiagonal random matrix that leads to the Dyson Brownian motions [HP17] and another that does not [Yab23]. Another attempt [ABG12, AG13] was restricted to a narrow range of the parameter $\beta \leq 2$.

This subtlety was recently settled and the general β -Dyson Brownian motions are certainly an eigenvalue process of a dynamical random matrix [HIM23]. Otherwise, if the Dyson Brownian motions do not have to be an eigenvalue process, we could interpret the previous work [KK21b] of the first two authors as providing a natural origin of Dyson Brownian motions in terms of the SLE/GFF-coupling.

As far as the authors are aware, the circular β -Dyson Brownian motions with general β have not been realized as an eigenvalue process of a dynamical random matrix though its static counterpart is an eigenvalue ensemble [DE02]. In this regard, we could say that the present work provides a natural origin of circular Dyson Brownian motions similarly to the chordal case.

Three phases of radial multiple SLE. In the previous work [KK21b] of the first two authors, we applied the coupling result to show that the multiple SLE exhibits three phases against the parameter κ . The three phases are well-known for the single curve SLE and can be transferred to the multiple SLE by absolute continuity of each curve with respect to the single curve SLE. However, the absolute continuity is only manifestly valid as long as the curves are apart from each other, i.e., when $\kappa \leq 4$. With our approach, we knew that there was a law of multiple curves determined by the GFF, and that allowed us to conclude the three phases for the larger range $\kappa \leq 8$.

We expect that the similar is true for the radial case, but the details are yet to be explored.

Other phase transitions. In the present work, we have seen that, at the hydrodynamic limit, the SLE hull $K_t^{[\infty]}$ changes its topology at $t = 1$. As we will see, this corresponds to the fact that the support of the circular Dyson Brownian motions at the hydrodynamic limit covers the entire \mathbb{S} . In some sense, we *upgraded* a phenomenon for the circular Dyson Brownian motions to the multiple SLE they drive.

There are a few intriguing phase transitions known for the circular Dyson Brownian motions at $\beta = 2$, also known as the non-intersecting Brownian motions. One example is [FMS11] (see also [MS14]) that studied the *normalized reunion probability* and found a third-order phase transition. Their method is remarkable; they matched the normalized reunion probability with the free energy of a Yang–Mills theory and transferred the known

result of phase transition due to [DK93]. Thus, their result is a version of the Gross–Witten–Wadia transition [GW80, Wad80] in random matrix theory.

Another phase transition is found in [LW16] that studied the non-intersecting Brownian motions on a circle conditioned to reunion after time T . They found that the widening number for those particles exhibits a critical phenomenon against T .

It is interesting to see if these other phase transitions can be *upgraded* to the multiple SLE.

Beyond hydrodynamic limit. Now that we understand the hydrodynamic limit of multiple SLE, a natural next question would be to see fluctuation in different scaling. The first result beyond the hydrodynamic limit appears in [CLM23] that studies the convergence rate in the chordal setting. We expect a similar result to hold in the radial case as well.

In random matrix theory, the Tracy–Widom distribution [TW94] for the properly scaled largest eigenvalue has been playing a prominent role in revealing universality. It would be interesting if we can lift the Tracy–Widom distribution to the multiple SLE, for example, by analysing the distribution of the right-most curve in a particular scaling.

Even further, we could go on to the large deviations. In fact, the third-order phase transition found in [FMS11, MS14] corresponds to the discrepancy between the left and right rate functions away from the critical value. Therefore, studying large deviations would be relevant for answering the questions posed in the above subsection. Also, the large deviation principles for the empirical measure of Dyson Brownian motions have been established in [GZ02, GH23]. Although it is unclear what is the analogue of the empirical measure for multiple SLE, it is interesting if multiple SLE admits a certain large deviation principle.

Though orthogonal to our setting of sending $N \rightarrow \infty$, we also would like to mention [PW23a, AHP24] that study the large deviation principles of multiple SLE as $\kappa \rightarrow 0$.

Multiply connected domains. The notion of SLE has been generalized to multiply connected domains [Zha04, Law06, BF06, BF08, Dre11, CFS17, CF18, Mur19]. On the other hand, the definition of GFF does not require that the domain is simply connected from the first place. In fact, coupling between these variants of SLE and GFF on multiply connected domains appeared in [IK13] on annuli and has been recently studied more in [BKT23, ABK24, AB24]. The present work encourages us to study the coupling in presence of multiple curves and derive a natural stochastic log-gas that arises in the boundaries of a multiply connected domain. This direction will be pursued in future work.

Organization of the paper. This paper is organized as follows. The following Section 2 provides a brief exposition of GFF. In Section 3, we discuss coupling between radial multiple SLE and GFF. This section contains the definition of coupling, a precise version of Theorem 1.4 as well as its proof. Finally, in Section 4, we describe the hydrodynamic limit of the radial multiple SLE driven by the circular Dyson Brownian motions.

Acknowledgments. MK, CS, and RS thank Taiki Endo and Miyu Ikegame for collaboration in the early stages of the study reported in Section 4. The authors are

grateful to Sebastian Schleißinger for informing them of the GitHub repository https://github.com/Sammy-Jankins/Complex_analysis, from which they adapted Python codes, and Saori Morimoto for useful discussion on numerical simulations that produced Figures 1 and 2. MK was supported by JSPS KAKENHI Grant Numbers JP21H04432, JP22H05105, JP23K25774, and JP24K06888. SK was supported by Academy of Finland (No. 248 130).

2. GAUSSIAN FREE FIELD

In this section, we introduce the necessary background on Gaussian free field (GFF). For more detailed account, see [She07, WP22, BP25].

2.1. Definition. Let $D \subset \mathbb{C}$ be a domain that has the Green's function $G_D(z, w)$ under the zero-boundary condition. Our convention is that the Green's function has the singularity

$$G_D(z, w) \sim -\log |z - w| \quad \text{as } z \rightarrow w.$$

Under this normalization, $\frac{1}{2\pi}G_D(z, w)$ is the integral kernel of the inverse of the Laplacian Δ^{-1} :

$$(2.1) \quad (-\Delta^{-1}f)(z) = \frac{1}{2\pi} \int_D G_D(z, w)f(w)\mathbf{m}(dw),$$

where $\mathbf{m}(dw) := d(\operatorname{Re} w)d(\operatorname{Im} w)$ is the Lebesgue measure on D induced from \mathbb{C} .

Example 2.1. We will need the Green's function on \mathbb{D} . It is given by

$$G_{\mathbb{D}}(z, w) = \log \left| \frac{z\bar{w} - 1}{z - w} \right|, \quad z, w \in \mathbb{D}.$$

Indeed, it has the correct singularity at $z = w$, is symmetric under exchanging z and w , and when $w \in \mathbb{S}$, we can see that $G_{\mathbb{D}}(z, w) = 0$ since $\bar{w} = w^{-1}$.

We write $C_0^\infty(D)$ for the space of smooth functions on D with compact support.

Definition 2.2. The zero-boundary GFF on D is a random distribution Γ with test functions in $C_0^\infty(D)$ such that $\Gamma(f)$, $f \in C_0^\infty(D)$ are centered Gaussian variables with covariance given by

$$\operatorname{Cov}(\Gamma(f), \Gamma(g)) = \int_{D \times D} f(z)G_D(z, w)g(w)\mathbf{m}(dz)\mathbf{m}(dw), \quad f, g \in C_0^\infty(D).$$

A non-trivial question is if a GFF even exists. We shall argue that it exists by sketching its construction. We start off by endowing $C_0^\infty(D)$ with the Dirichlet inner product

$$(f, g)_\nabla = \frac{1}{2\pi} \int_D (\nabla f)(z) \cdot (\nabla g)(z)\mathbf{m}(dz), \quad f, g \in C_0^\infty(D).$$

The Hilbert space completion of $C_0^\infty(D)$ with respect to this inner product will be denoted by $W(D)$. For a complete orthonormal system $\{\mathbf{w}_i\}_i$ of $W(D)$, we consider the following infinite sum

$$(2.2) \quad \Gamma = \sum_i \alpha_i \mathbf{w}_i, \quad \alpha_i \sim N(0, 1) : \text{i.i.d.}$$

It is clear that Γ converges in $W(D)$ with zero-probability. The hardest part of the construction of a GFF is that Γ almost surely converges as a distribution with test functions in $C_0^\infty(D)$. We do not give a complete proof of this part, but just mention that it relies on Weyl's law for the spectrum of the Laplacian. See [She07] for detail.

Once we know that Γ converges as a distribution, it is clear that $\Gamma(f)$, $f \in C_0^\infty(D)$ are centered Gaussian variables. It remains to see that they exhibit the correct covariance.

Proposition 2.3. *The covariance of the centered Gaussian variables $\Gamma(f)$, $f \in C_0^\infty(D)$ are given by*

$$\text{Cov}(\Gamma(f), \Gamma(g)) = \int_{D \times D} f(z) G_D(z, w) g(w) \mathbf{m}(dz) \mathbf{m}(dw), \quad f, g \in C_0^\infty(D).$$

Proof. Since the assignment $f \mapsto \Gamma(f)$ is linear, it suffices to check that each $\Gamma(f)$, $f \in C_0^\infty(D)$ exhibits the variance

$$\text{Var}(\Gamma(f)) = \int_{D \times D} f(z) G_D(z, w) f(w) \mathbf{m}(dz) \mathbf{m}(dw).$$

Since $\{\mathbf{w}_i\}_i$ is orthonormal with respect to the Dirichlet inner product, by integration by parts, we can see

$$\delta_{i,j} = (\mathbf{w}_i, \mathbf{w}_j)_\nabla = \frac{-1}{2\pi} (\mathbf{w}_i, \Delta \mathbf{w}_j),$$

which implies that $\{(\frac{-1}{2\pi} \Delta) \mathbf{w}_i\}_i$ is the dual basis of $\{\mathbf{w}_i\}_i$ with respect to the L^2 -pairing. Let us expand $f \in C_0^{(\infty)}(D)$ in terms of $\{(\frac{-1}{2\pi} \Delta) \mathbf{w}_i\}_i$:

$$f = \sum_i f_i \left(\frac{-1}{2\pi} \Delta \right) \mathbf{w}_i.$$

Then, we obtain

$$\Gamma(f) = \sum_i \alpha_i f_i,$$

from which we get

$$\text{Var}(\Gamma(f)) = \sum_i f_i^2.$$

By definition, each f_i is given by

$$f_i = (f, \mathbf{w}_i) = ((-2\pi \Delta^{-1}) f, \mathbf{w}_i)_\nabla,$$

which leads to

$$\text{Var}(\Gamma(f)) = \|(-2\pi \Delta^{-1}) f\|_\nabla^2.$$

By integration by parts, we obtain the desired result:

$$\text{Var}(\Gamma(f)) = 2\pi \int_D ((-\Delta)^{-1} f)(z) f(z) dz = \int_{D \times D} f(z) G(z, w) f(w) \mathbf{m}(dz) \mathbf{m}(dw),$$

where we also used (2.1). □

More generally, we refer to the sum of the zero-boundary GFF and a deterministic harmonic function as a GFF. Since a harmonic function is determined by its boundary values, this is to impose boundary conditions on the GFF.

2.2. Domain Markov property. Let us suppose that $D \subset \mathbb{C}$ is a domain as above and Γ_D is a Dirichlet boundary GFF on D . Note that, since Γ_D is a distribution on D , we can restrict it to a subdomain. The domain Markov property of GFF refers to the following property.

Proposition 2.4. *Let us pick a subdomain $U \subset D$. Then, conditioned over $D \setminus U$,*

$$\Gamma_D|_U = \Gamma_U + \mathbf{u},$$

where \mathbf{u} is the harmonic extension of $\Gamma_D|_{\partial U}$ in U .

We only give heuristics instead of a complete proof. Note that, when we embed $W(U)$ in $W(D)$, the orthogonal complement $W(U)^\perp$ consists of those in $W(D)$ that are harmonic on U . We may pick complete orthonormal systems of $W(U)$ and $W(U)^\perp$ and combine them to get one of $W(D)$. Therefore, the infinite-sum (2.2) decomposes into mutually independent parts as

$$\Gamma_D = \Gamma_U + \Gamma_U^h,$$

where Γ_U is a Dirichlet boundary GFF on U , extended as zero outside U , and Γ_U^h is harmonic on U . When conditioned over $D \setminus U$ and restricted on U , Γ_U remains as is and $\mathbf{u} = \Gamma_U^h|_U$ gives a harmonic extension of $\Gamma_D|_{\partial U}$ on U .

From the above explanation, we can see that the harmonic function \mathbf{u} in Proposition 2.4 can be extracted as a conditional expectation. We write $\mathcal{F}_{(D \setminus U)^+}$ for the σ -algebra generated by Γ projected to $W(U)^\perp$. Since Γ_U is centered, we have

$$\mathbf{u} = \mathbb{E}[\Gamma_D|_U | \mathcal{F}_{(D \setminus U)^+}].$$

This observation will be used later.

3. COUPLING

In this section, we discuss coupling between radial multiple SLE and GFF, and present our first main result; Theorem 3.4, the precise version of Theorem 1.4.

3.1. Motivating example: single-curve case. Coupling between radial SLE and GFF has been studied in [IK13] in the case that the SLE parameter is $\kappa = 4$. To motivate our setting with radial multiple SLE, let us first formulate the result for the single-curve case. (This would also be useful as computational warm-up.)

Let $\kappa > 0$ and $(g_t : t \geq 0)$ be the radial SLE driven by $(X_t = e^{i\sqrt{\kappa}B_t} : t \geq 0)$, where $(B_t : t \geq 0)$ is a standard Brownian motion, i.e., it is the solution to (1.3). Recall that, at each $t \geq 0$, we may find a domain $\mathbb{D}_t \subset \mathbb{D}$ that is conformally mapped to \mathbb{D} by g_t . At each $t \geq 0$, we define the harmonic function \mathbf{u}_t on \mathbb{D}_t by

$$(3.1) \quad \mathbf{u}_t(z) = -\frac{2}{\sqrt{\kappa}} \arg(g_t(z) - X_t) + \xi_1 \arg(g_t(z)) - \chi \arg(g'_t(z)) + B_t, \quad z \in \mathbb{D}_t,$$

where $\xi_1 = \frac{3}{\sqrt{\kappa}} - \frac{\sqrt{\kappa}}{2}$ and $\chi = \frac{2}{\sqrt{\kappa}} - \frac{\sqrt{\kappa}}{2}$. Note that \mathbf{u}_t is not single valued due to the presence of $\arg(g_t(z))$ and $\arg(g'_t(z))$. Nevertheless, we argue that \mathbf{u}_t is the natural generalization of the harmonic function that was used to construct a coupling of chordal SLE and GFF.

Let $U \subset \mathbb{D}$ be an open set and define the stopping time

$$(3.2) \quad \tau_U = \sup\{t \geq 0 \mid U \subset \mathbb{D}_t\}.$$

For a stopping time τ such that $\mathbb{P}[\tau \leq \tau_U] = 1$, we define the GFF $h_{U,\tau}$ on U by first sampling \mathbb{D}_τ and then setting

$$(3.3) \quad h_{U,\tau} = (\Gamma_{\mathbb{D}_\tau} + \mathbf{u}_\tau)|_U.$$

The following theorem has been proved in [IK13] in the case that $\kappa = 4$.

Theorem 3.1. *For any open set $U \subset \mathbb{D}$ and a stopping time τ such that $\mathbb{P}[\tau \leq \tau_U] = 1$, we have*

$$h_{U,\tau} \stackrel{(\text{law})}{=} h_{U,0}.$$

Remark 3.2. The last term B_t in (3.1) is missing from the harmonic function used in [IK13]. This is necessary for the coupling in Theorem 3.1 to our understanding.

Remark 3.3. It is common to formulate coupling between SLE and GFF as local set coupling. In this regard, we could state that $K_\tau = \mathbb{D} \setminus \mathbb{D}_\tau$ is a local set for $\Gamma_{\mathbb{D}} + \mathbf{u}_0$ (see [MS16a] for the definition). Although the local set coupling is stronger than Theorem 3.1, we shall not fill this gap as the proof would be very similar to the chordal case [MS16a], provided Theorem 3.1.

Proof of Theorem 3.1. First, we show that, for each $z \in \mathbb{D}$, the process $(\mathbf{u}_t(z) : 0 \leq t \leq \tau_z)$ is a local martingale. Here, τ_z is the stopping time until which the solution $g_t(z)$ exists. For computational convenience, we shall note that $\mathbf{u}_t(z) = \text{Im} \tilde{\mathbf{u}}_t(z)$ with

$$\tilde{\mathbf{u}}_t(z) = -\frac{2}{\sqrt{\kappa}} \log(g_t(z) - X_t) + \xi_1 \log(g_t(z)) - \chi \log(g'_t(z)) + \mathbf{i} B_t.$$

Let us execute Ito calculus. The circular Brownian motion $(X_t : t \geq 0)$ satisfies

$$dX_t = \mathbf{i} \sqrt{\kappa} X_t dB_t - \frac{\kappa}{2} X_t dt.$$

Introducing the function

$$(3.4) \quad \Psi(z, x) = -z \frac{z+x}{z-x}, \quad z \in \mathbb{D}, x \in \mathbb{S},$$

the radial Loewner equation reads

$$\frac{d}{dt} g_t(z) = \Psi(g_t(z), X_t).$$

It will be computationally useful to have the Laurent expansion of $\Psi(z, x)$ at $z = x$:

$$(3.5) \quad \Psi(z, x) = -\frac{2x^2}{z-x} - 3x - (z-x).$$

Let us start by computing the increment of $\log(g_t(z) - X_t)$:

$$\begin{aligned} d\log(g_t(z) - X_t) &= \frac{d(g_t(z) - X_t)}{g_t(z) - X_t} - \frac{1}{2} \frac{d\langle X_t, X_t \rangle}{(g_t(z) - X_t)^2} \\ &= \frac{-\mathfrak{i}\sqrt{\kappa}X_t}{g_t(z) - X_t} dB_t + K_1(g_t(z), X_t)dt, \end{aligned}$$

where

$$\begin{aligned} K_1(z, x) &= \frac{\Psi(z, x)}{z - x} + \frac{\kappa}{2} \frac{x}{z - x} + \frac{\kappa}{2} \frac{x^2}{(z - x)^2} \\ &= \frac{(\frac{\kappa}{2} - 2)x^2}{(z - x)^2} + \frac{(\frac{\kappa}{2} - 3)x}{z - x} - 1. \end{aligned}$$

The second and third terms of $\tilde{\mathbf{u}}_t(z)$ are purely drift terms: we obtain

$$\frac{d}{dt} \log(g_t(z)) = \frac{1}{g_t(z)} \frac{d}{dt} g_t(z) = L_1(g_t(z), X_t)$$

with

$$L_1(z, x) = \frac{1}{z} \Psi(z, x) = -\frac{z + x}{z - x} = -\frac{2x}{z - x} - 1$$

and

$$\frac{d}{dt} \log(g'_t(z)) = \frac{1}{g'_t(z)} \frac{d}{dt} g'_t(z) = \frac{\partial \Psi}{\partial z}(g_t(z), X_t) = M_1(g_t(z), X_t)$$

with

$$M_1(z, x) = \frac{\partial \Psi}{\partial z}(z, x) = \frac{2x^2}{(z - x)^2} - 1.$$

We shall observe that

$$\begin{aligned} & -\frac{2}{\sqrt{\kappa}} K_1(z, x) + \xi_1 L_1(z, x) - \chi M_1(z, x) \\ &= \frac{-2(\chi - (\frac{2}{\sqrt{\kappa}} - \frac{\sqrt{\kappa}}{2}))x^2}{(z - x)^2} + \frac{-2(\xi_1 - (\frac{3}{\sqrt{\kappa}} - \frac{\sqrt{\kappa}}{2}))x}{z - x} + \frac{2}{\sqrt{\kappa}} - \xi_1 + \chi \end{aligned}$$

is a real constant if $\chi = \frac{2}{\sqrt{\kappa}} - \frac{\sqrt{\kappa}}{2}$ and $\xi_1 = \frac{3}{\sqrt{\kappa}} - \frac{\sqrt{\kappa}}{2}$. Therefore, under these choices of ξ_1 and χ , $(\mathbf{u}_t(z) : 0 \leq t \leq \tau_z)$ is a local martingale:

$$\begin{aligned} d\mathbf{u}_t(z) &= -\frac{2}{\sqrt{\kappa}} \operatorname{Im} \left(\frac{-\mathfrak{i}\sqrt{\kappa}X_t}{g_t(z) - X_t} \right) dB_t + dB_t = \operatorname{Im} \left(\mathfrak{i} \frac{g_t(z) + X_t}{g_t(z) - X_t} \right) dB_t \\ &= \operatorname{Re} \left(\frac{g_t(z) + X_t}{g_t(z) - X_t} \right) dB_t. \end{aligned}$$

Next, we pick $z, w \in \mathbb{D}$ and relate the quadratic variation $\langle \mathbf{u}_t(z), \mathbf{u}_t(w) \rangle$ to the Green's function of \mathbb{D}_t . From the above computation, we have

$$\frac{d}{dt} \langle \mathbf{u}_t(z), \mathbf{u}_t(w) \rangle = \operatorname{Re} \left(\frac{g_t(z) + X_t}{g_t(z) - X_t} \right) \operatorname{Re} \left(\frac{g_t(w) + X_t}{g_t(w) - X_t} \right), \quad 0 \leq t \leq \tau_z \wedge \tau_w.$$

For the Green's function, we have $G_{\mathbb{D}_t}(z, w) = G_{\mathbb{D}}(g_t(z), g_t(w))$, and from Example 2.1,

$$\frac{d}{dt}G_{\mathbb{D}_t}(z, w) = \Pi_1(g_t(z), g_t(w); X_t)$$

with

$$(3.6) \quad \Pi_1(z, w; x) = \operatorname{Re} \frac{-1}{1 - z\bar{w}} \left(\Psi(z, x)\bar{w} + z\overline{\Psi(w, x)} \right) + \operatorname{Re} \frac{-1}{z - w} (\Psi(z, x) - \Psi(w, x)).$$

By direct computation, we can see that

$$\Psi(z, x)\bar{w} + z\overline{\Psi(w, x)} = (1 - z\bar{w}) \frac{2z\bar{w}}{(z - x)(\bar{w} - \bar{x})},$$

where we used $|x| = 1$ for $x \in \mathbb{S}$ and

$$\Psi(z, x) - \Psi(w, x) = (z - w) \left(\frac{z + x}{z - x} \frac{w + x}{w - x} - \frac{2zw}{(z - x)(w - x)} \right).$$

We can immediately notice that, in $\Pi_1(z, w; x)$, there is a contribution of the form

$$\begin{aligned} \operatorname{Re} \left(\frac{z}{z - x} \left(\frac{2w}{w - x} - \frac{2\bar{w}}{\bar{w} - \bar{x}} \right) \right) &= \operatorname{Re} \left(\frac{2z}{z - x} \right) \operatorname{Im} \left(\frac{2w}{w - x} \right) \\ &= -\operatorname{Im} \left(\frac{2z}{z - x} \right) \operatorname{Im} \left(\frac{2w}{w - x} \right). \end{aligned}$$

Hence, we obtain

$$\Pi_1(z, w; x) = -\operatorname{Im} \left(\frac{2z}{z - x} \right) \operatorname{Im} \left(\frac{2w}{w - x} \right) - \operatorname{Re} \left(\frac{z + x}{z - x} \frac{w + x}{w - x} \right).$$

As far as the imaginary part is concerned, we have

$$\operatorname{Im} \left(\frac{2z}{z - x} \right) = \operatorname{Im} \left(\frac{z + x}{z - x} \right).$$

Thus, we get

$$(3.7) \quad \Pi_1(z, w; x) = -\operatorname{Re} \left(\frac{z + x}{z - x} \right) \operatorname{Re} \left(\frac{w + x}{w - x} \right),$$

which allows us to conclude that

$$(3.8) \quad \langle \mathbf{u}_t(z), \mathbf{u}_t(w) \rangle + G_{\mathbb{D}_t}(z, w) = G_{\mathbb{D}}(z, w), \quad 0 \leq t \leq \tau_z \wedge \tau_w.$$

Now, we pick an open set $U \subset \mathbb{D}$ and a test function $f \in C_0^\infty(\mathbb{D})$ such that $\operatorname{supp}(f) \subset U$, we have

$$\langle (\mathbf{u}_t, f), (\mathbf{u}_t, f) \rangle + E_{\mathbb{D}_t}(f) = E_{\mathbb{D}}(f), \quad 0 \leq t \leq \tau_U,$$

where

$$E_{\mathbb{D}_t}(f) = \int_{\mathbb{D}_t \times \mathbb{D}_t} f(z) G_{\mathbb{D}_t}(z, w) f(w) \mathbf{m}(dz) \mathbf{m}(dw)$$

is the Dirichlet energy of f in \mathbb{D}_t . Though this is a direct consequence of (3.8) and Fubini's theorem, applying Fubini's theorem requires a slight care. We do not provide the details here as the argument is the same as [MS16a, Section 3.3].

Let us write $(\mathcal{F}_t)_{t \geq 0}$ for the filtration to which the radial SLE is adapted. For any stopping time τ such that $\mathbb{P}[\tau \leq \tau_U] = 1$, \mathbf{u}_τ is measurable with respect to \mathcal{F}_τ . Therefore, we have

$$\begin{aligned} \mathbb{E}[e^{i\theta(h_{U,\tau},f)}] &= \mathbb{E}\left[\mathbb{E}[e^{i\theta(\Gamma_{\mathbb{D}_\tau},f)}|\mathcal{F}_\tau]e^{i\theta(\mathbf{u}_\tau,f)}\right] \\ &= \mathbb{E}\left[e^{i\theta(\mathbf{u}_\tau,f) - \frac{\theta^2}{2}E_{\mathbb{D}_\tau}(f)}\right] \\ &= \mathbb{E}\left[e^{i\theta(\mathbf{u}_0,f) - \frac{\theta^2}{2}E_{\mathbb{D}}(f)}\right] \\ &= \mathbb{E}[e^{i\theta(h_{U,0},f)}], \quad \theta \in \mathbb{R}, \end{aligned}$$

as is desired. \square

3.2. Multiple curve case. We now consider coupling of radial multiple SLE and GFF. Let $N \geq 1$ and $(g_t : t \geq 0)$ be the radial multiple SLE with continuous driving processes $(X_t^{(i)} = e^{i\Theta_t^{(i)}} : t \geq 0)$, $i = 1, \dots, N$, i.e., it is the solution of (1.4). In contrast to the previous section, we have not fixed the law of the driving processes. We write T for the collision time of the driving processes that could be finite with positive probability.

To formulate our result, we first need to postulate an analogue of (3.1) when there are multiple driving processes. The harmonic function (3.1) imposes the boundary condition that has a jump at $g_t(z) = X_t$ by $-\frac{2}{\sqrt{\kappa}}$ and an additive constant fluctuation by B_t . In the presence of multiple driving processes $(X_t^{(i)} : t \geq 0)$, $i = 1, \dots, N$, it would be natural if the boundary value jumps at every $g_t(z) = X_t^{(i)}$, $i = 1, \dots, N$. For the constant fluctuation, we postulate $\sum_{i=1}^N \Theta_t^{(i)}$. That is, we fix $\kappa > 0$, $\xi, \chi, \zeta \in \mathbb{R}$, and, at each $t \geq 0$, we take the harmonic function

$$\mathbf{u}_t^{(N)}(z) = -\frac{2}{\sqrt{\kappa}} \sum_{i=1}^N \arg(g_t(z) - X_t^{(i)}) + \xi \arg(g_t(z)) - \chi \arg(g'_t(z)) + \zeta \sum_{i=1}^N \Theta_t^{(i)}$$

of $z \in \mathbb{D}_t$. Note that the four parameters κ, ξ, χ and ζ are not yet related.

Next, we define the coupling. For an open set $U \subset \mathbb{D}$, the stopping time τ_U is given by

$$\tau_U = \sup\{t \geq 0 | U \subset \mathbb{D}_t\} \wedge T.$$

This is almost same as (3.2) except we cannot continue the process after collision of the driving processes at time T . For a stopping time τ such that $\mathbb{P}[\tau \leq \tau_U] = 1$, the GFF $h_{U,\tau}$ is sampled in the same way as (3.3) except that we use the harmonic function $\mathbf{u}_\tau^{(N)}$ instead. To be precise, we first sample \mathbb{D}_τ , and put

$$h_{U,\tau} = (\Gamma_{\mathbb{D}_\tau} + \mathbf{u}_\tau^{(N)})|_U.$$

The main result in this section goes as follows.

Theorem 3.4. *The following are equivalent:*

(1) for any open set $U \subset \mathbb{D}$ and a stopping time τ such that $\mathbb{P}[\tau \leq \tau_U] = 1$, we have

$$h_{U,\tau} \stackrel{(\text{law})}{=} h_{U,0},$$

(2) the driving processes satisfy the system of SDEs (1.5), $\xi_N = \frac{N+2}{\sqrt{\kappa}} - \frac{\sqrt{\kappa}}{2}$, $\chi = \frac{2}{\sqrt{\kappa}} - \frac{\sqrt{\kappa}}{2}$, and $\zeta = \frac{1}{\sqrt{\kappa}}$.

Remark 3.5. Theorem 3.4 is, in fact, a generalization of Theorem 3.1 in two ways. For the one, Theorem 3.4 covers the case that $N \geq 1$, but it also says that coupling uniquely fix driving processes and the parameters ξ_N and χ .

Remark 3.6. The circular β -Dyson Brownian motions almost surely do not collide when $\beta \geq 1$, and they almost surely collide when $0 < \beta < 1$. So, the collision time T is, in fact, almost surely infinite for the former case, and finite for the latter case.

Proof. We only prove that (1) implies (2). Once we understand it, the other direction goes by straightforward computation and similar arguments as the single-curve case.

Let us first pick an open set $U \subset \mathbb{D}$ and a stopping time τ such that $\mathbb{P}[\tau \leq \tau_U] = 1$. By the domain Markov property of GFF, conditioned over $K_\tau = \mathbb{D} \setminus \mathbb{D}_\tau$, we know that the harmonic function \mathbf{u}_τ is extracted as

$$\mathbf{u}_\tau^{(N)} = \mathbb{E}[h_{U,0} | \mathcal{F}_{K_\tau^+}].$$

Let us take test functions $f_1, f_2 \in C_0^\infty(\mathbb{D})$ such that $\text{supp}(f_i) \subset U$, $i = 1, 2$. Then, we know that $(h_{U,0}, f_i)$, $i = 1, 2$ are Gaussian variables of covariance

$$\int_{\mathbb{D} \times \mathbb{D}} f_1(z) G_{\mathbb{D}}(z, w) f_2(w) \mathbf{m}(dz) \mathbf{m}(dw).$$

By the coupling, sampling them is equivalent to sampling $(\Gamma_{\mathbb{D}_\tau}, f_i)$, $i = 1, 2$ and add to them $(\mathbf{u}_\tau^{(N)}, f_i)$, $i = 1, 2$ that are, due to the domain Markov property, conditionally independent of $\Gamma_{\mathbb{D}_\tau}$ given K_τ . Therefore, the covariance of the Gaussian variables $(\mathbf{u}_\tau^{(N)}, f_i)$, $i = 1, 2$ is given by

$$\int_{\mathbb{D} \times \mathbb{D}} f_1(z) (G_{\mathbb{D}}(z, w) - G_{\mathbb{D}_\tau}(z, w)) f_2(w) \mathbf{m}(dz) \mathbf{m}(dw).$$

Now, for $z \in \mathbb{D}$, we take a sequence of open sets U_i , $i \in \mathbb{N}$ such that $\bigcap_{i \in \mathbb{N}} U_i = \{z\}$. For each $i \in \mathbb{N}$, the process $(\mathbf{u}_{t \wedge \tau_{U_i}}^{(N)}(z) : t \geq 0)$ is a martingale. Since $\tau_{U_i} \rightarrow \tau_z$ as $i \rightarrow \infty$, we have that $(\mathbf{u}_{t \wedge \tau_z}^{(N)}(z) : t \geq 0)$ is a local martingale. Similarly, for $z, w \in \mathbb{D}$, we take a sequence of open sets U_i , $i \in \mathbb{N}$ such that $\bigcap_{i \in \mathbb{N}} U_i = \{z, w\}$ to see that

$$\langle \mathbf{u}_{t \wedge \tau_{U_i}}^{(N)}(z), \mathbf{u}_{t \wedge \tau_{U_i}}^{(N)}(w) \rangle = G_{\mathbb{D}}(z, w) - G_{\mathbb{D}_{t \wedge \tau_{U_i}}}(z, w).$$

Note that the right-hand side makes sense at $z = w$ though each Green's function does not. At the limit $i \rightarrow \infty$, we get

$$d \langle \mathbf{u}_t^{(N)}(z), \mathbf{u}_t^{(N)}(w) \rangle = -dG_{\mathbb{D}_t}(z, w), \quad 0 \leq t \leq \tau_z \wedge \tau_w.$$

We have just observed that $(\mathbf{u}_t^{(N)}(z) : t \in [0, \tau_z])$ is a local martingale for any $z \in \mathbb{D}$. When we take generic points z_1, \dots, z_N , we can write each $\Theta_t^{(i)}$ as a smooth function of $\mathbf{u}_t^{(N)}(z_j)$, $g_t(z_j)$, and $g'_t(z_j)$, $j = 1, \dots, N$ due to the implicit function theorem. This implies that each $(\Theta_t^{(i)} : t \geq 0)$ is a semi-martingale admitting a decomposition

$$(3.9) \quad \Theta_t^{(i)} = \mathbf{M}_t^{(i)} + \mathbf{U}_t^{(i)},$$

where $\mathbf{M}_t^{(i)}$ is the martingale and $\mathbf{U}_t^{(i)}$ is the drift part of $\Theta_t^{(i)}$.

We set

$$\widetilde{\mathbf{u}}_t^{(N)}(z) = -\frac{2}{\sqrt{\kappa}} \sum_{i=1}^N \log(g_t(z) - X_t^{(i)}) + \xi \log(g_t(z)) - \chi \log(g'_t(z)) + \mathbf{i}\zeta \sum_{i=1}^N \Theta_t^{(i)}$$

so that $\mathbf{u}_t^{(N)}(z) = \text{Im} \widetilde{\mathbf{u}}_t^{(N)}(z)$. Since $\widetilde{\mathbf{u}}_t^{(N)}(z)$ is holomorphic in z , its real and imaginary parts are related by the Cauchy–Riemann identities. Therefore, the drift term of $\widetilde{\mathbf{u}}_t^{(N)}(z)$ must be purely real.

Using the decomposition (3.9) we can compute the increment of $\widetilde{\mathbf{u}}_t^{(N)}(z)$ by Ito's formula. Computation is very similar to that in the proof of Theorem 3.1 except that we do not know explicit forms of $\mathbf{M}_t^{(i)}$ and $\mathbf{U}_t^{(i)}$ at this point. Let us start with each of the driving processes $(X_t^{(i)} : t \geq 0)$, $i = 1, \dots, N$:

$$dX_t^{(i)} = \mathbf{i}X_t^{(i)} d\mathbf{M}_t^{(i)} + \left(\mathbf{i} \frac{d\mathbf{U}_t^{(i)}}{dt} - \frac{1}{2} \frac{d\langle \mathbf{M}_t^{(i)}, \mathbf{M}_t^{(i)} \rangle}{dt} \right) dt.$$

The Loewner equation reads

$$\frac{d}{dt} g_t(z) = \sum_{i=1}^N \Psi(g_t(z), X_t^{(i)})$$

with the same function $\Psi(z, x)$ in (3.4). Thus, we can first compute, for each $i = 1, \dots, N$,

$$(3.10) \quad \begin{aligned} d \log(g_t(z) - X_t^{(i)}) &= \frac{d(g_t(z) - X_t^{(i)})}{g_t(z) - X_t^{(i)}} + \frac{(X_t^{(i)})^2}{2(g_t(z) - X_t^{(i)})^2} d\langle \mathbf{M}_t^{(i)}, \mathbf{M}_t^{(i)} \rangle \\ &= \frac{-\mathbf{i}X_t^{(i)}}{g_t(z) - X_t^{(i)}} d\mathbf{M}_t^{(i)} + K_t^{(i)}(g_t(z), X_t^{(i)}) dt, \end{aligned}$$

where

$$\begin{aligned} K_t^{(i)}(z, \mathbf{x}) &= \frac{1}{z - x_i} \sum_{j=1}^N \Psi(z, x_j) - \frac{x_i}{z - x_i} \left(\mathbf{i} \frac{d\mathbf{U}_t^{(i)}}{dt} - \frac{1}{2} \frac{d\langle \mathbf{M}_t^{(i)}, \mathbf{M}_t^{(i)} \rangle}{dt} \right) \\ &\quad + \frac{x_i^2}{2(z - x_i)^2} \frac{d\langle \mathbf{M}_t^{(i)}, \mathbf{M}_t^{(i)} \rangle}{dt}. \end{aligned}$$

We prepare here a small technical lemma.

Lemma 3.7. *We have the following identity of rational functions of z :*

$$\sum_{i,j=1}^N \frac{\Psi(z, x_j)}{z - x_i} = \sum_{i=1}^N \frac{-2x_i^2}{(z - x_i)^2} + \sum_{i=1}^N \frac{-x_i}{z - x_i} \left(2 \sum_{\substack{j=1 \\ j \neq i}}^N \frac{x_i + x_j}{x_i - x_j} + N + 2 \right) - N^2.$$

Proof. The diagonal sum immediately becomes

$$(3.11) \quad \sum_{i=1}^N \frac{\Psi(z, x_i)}{z - x_i} = \sum_{i=1}^N \left(-\frac{2x_i^2}{(z - x_i)^2} - \frac{3x_i}{z - x_i} \right) - N$$

due to the Laurent expansion (3.5). The off-diagonal sum

$$- \sum_{\substack{i,j=1 \\ i \neq j}}^N \frac{z}{z - x_i} \frac{z + x_j}{z - x_j}$$

converges to $-N(N-1)$ as $z \rightarrow \infty$ and has simple poles at $z = x_i$, $i = 1, \dots, N$. Hence, it admits the partial fraction decomposition:

$$(3.12) \quad - \sum_{\substack{i,j=1 \\ i \neq j}}^N \frac{z}{z - x_i} \frac{z + x_j}{z - x_j} = \sum_{i=1}^N \frac{-x_i}{z - x_i} \left(\sum_{\substack{j=1 \\ j \neq i}}^N \frac{x_i + x_j}{x_i - x_j} + \sum_{\substack{j=1 \\ j \neq i}}^N \frac{2x_i}{x_i - x_j} \right) - N(N-1) \\ = \sum_{i=1}^N \frac{-x_i}{z - x_i} \left(2 \sum_{\substack{j=1 \\ j \neq i}}^N \frac{x_i + x_j}{x_i - x_j} + N - 1 \right) - N(N-1).$$

Combining (3.11) and (3.12), we obtain the desired identity. \square

We then sum up (3.10) over $i = 1, \dots, N$ to have

$$\sum_{i=1}^N d \log(g_t(z) - X_t^{(i)}) = \sum_{i=1}^N \frac{-\mathbf{i} X_t^{(i)}}{g_t(z) - X_t^{(i)}} d\mathbf{M}_t^{(i)} + K_{N,t}(g_t(z), \mathbf{X}_t),$$

where

$$K_{N,t}(z, \mathbf{x}) = \sum_{i=1}^N K_t^{(i)}(z, x_i) \\ = \sum_{i=1}^N \left\{ \frac{x_i^2}{(z - x_i)^2} \left(-2 + \frac{1}{2} \frac{d \langle \mathbf{M}_t^{(i)}, \mathbf{M}_t^{(i)} \rangle}{dt} \right) \right. \\ \left. + \frac{-x_i}{z - x_i} \left(\mathbf{i} \frac{d\mathbf{U}_t^{(i)}}{dt} - \frac{1}{2} \frac{d \langle \mathbf{M}_t^{(i)}, \mathbf{M}_t^{(i)} \rangle}{dt} + 2 \sum_{\substack{j=1 \\ j \neq i}}^N \frac{x_i + x_j}{x_i - x_j} + N + 2 \right) \right\} \\ - N^2.$$

Both $\log(g_t(z))$ and $\log(g'_t(z))$ are easier to handle as they only have drift terms. In fact, we obtain

$$\frac{d}{dt} \log(g_t(z)) = L_N(g_t(z), \mathbf{X}_t)$$

with

$$L_N(z, \mathbf{x}) = \sum_{i=1}^N \frac{1}{z} \Psi(z, x_i) = \sum_{i=1}^N \frac{-2x_i}{z - x_i} - N$$

and

$$\frac{d}{dt} \log(g'_t(z)) = M_N(g_t(z), \mathbf{X}_t)$$

with

$$M_N(z, \mathbf{x}) = \sum_{i=1}^N \frac{\partial \Psi}{\partial z}(z, x_i) = \sum_{i=1}^N \frac{2x_i^2}{(z - x_i)^2} - N.$$

Combining the above computation altogether, we get

$$\begin{aligned} & d\tilde{\mathbf{u}}_t^{(N)}(z) \\ &= \frac{\mathfrak{i}}{\sqrt{\kappa}} \sum_{i=1}^N \left(\frac{2X_t^{(i)}}{g_t(z) - X_t^{(i)}} + \sqrt{\kappa}\zeta \right) d\mathbf{M}_t^{(i)} \\ &+ \left(-\frac{2}{\sqrt{\kappa}} K_{N,t}(g_t(z), \mathbf{X}_t) + \xi L_N(g_t(z), \mathbf{X}_t) - \chi M_N(g_t(z), \mathbf{X}_t) + \frac{\mathfrak{i}}{\sqrt{\kappa}} \sum_{i=1}^N \frac{d\mathbf{U}_t^{(i)}}{dt} \right) dt. \end{aligned}$$

Let us look at the pole of order 2 at $z = x_i$ in the drift term of $d\tilde{\mathbf{u}}_t^{(N)}(z)$. Since the residue must vanish, we have

$$-\frac{2}{\sqrt{\kappa}} \left(-2 + \frac{1}{2} \frac{d \langle \mathbf{M}_t^{(i)}, \mathbf{M}_t^{(i)} \rangle}{dt} \right) - 2\chi = 0.$$

By introducing $\lambda = \frac{2}{\sqrt{\kappa}} \left(\frac{2}{\sqrt{\kappa}} - \frac{\sqrt{\kappa}}{2} - \chi \right)$, we can solve it as

$$\langle \mathbf{M}_t^{(i)}, \mathbf{M}_t^{(i)} \rangle = \kappa(1 + \lambda)t, \quad t \geq 0.$$

Using this in the first order pole at $z = x_i$, we can see that we must have

$$\frac{2}{\sqrt{\kappa}} \left(\mathfrak{i} \frac{d\mathbf{U}_t^{(i)}}{dt} - \frac{\kappa}{2}(1 + \lambda) + 2 \sum_{\substack{j=1 \\ j \neq i}}^N \frac{x_i + x_j}{x_i - x_j} + N + 2 \right) - 2\xi = 0.$$

Since $x_i \in \mathbb{S}$, $i = 1, \dots, N$, the fraction $\frac{x_i + x_j}{x_i - x_j}$ is purely imaginary for all pairs $i \neq j$. Thus, the imaginary part of the above equation gives

$$\frac{d\mathbf{U}_t^{(i)}}{dt} = F^{(i)}(\mathbf{X}_t), \quad F^{(i)}(\mathbf{x}) := 2\mathfrak{i} \sum_{\substack{j=1 \\ j \neq i}}^N \frac{x_i + x_j}{x_i - x_j}, \quad t \geq 0$$

and the real part

$$\xi = \frac{N+2}{\sqrt{\kappa}} - \frac{\sqrt{\kappa}}{2}(1+\lambda).$$

Under this choice of the drift terms $U_t^{(i)}$, $i = 1, \dots, N$, we have $\sum_{i=1}^N \frac{dU_t^{(i)}}{dt} = 0$. Hence, the increment of $u_t^{(N)}(z)$ reads

$$du_t^{(N)}(z) = \frac{1}{\sqrt{\kappa}} \sum_{i=1}^N \operatorname{Re} \left(\frac{2X_t^{(i)}}{g_t(z) - X_t^{(i)}} + \sqrt{\kappa}\zeta \right) dM_t^{(i)}.$$

The cross variation between $u_t^{(N)}(z)$ and $u_t^{(N)}(w)$ is thus computed as

$$\begin{aligned} & d \langle u_t^{(N)}(z), u_t^{(N)}(w) \rangle \\ &= (1+\lambda) \sum_{i=1}^N \operatorname{Re} \left(\frac{g_t(z) + X_t^{(i)}}{g_t(z) - X_t^{(i)}} + (\sqrt{\kappa}\zeta - 1) \right) \operatorname{Re} \left(\frac{g_t(w) + X_t^{(i)}}{g_t(w) - X_t^{(i)}} + (\sqrt{\kappa}\zeta - 1) \right) dt \\ &+ \frac{1}{\kappa} \sum_{i \neq j} \operatorname{Re} \left(\frac{2X_t^{(i)}}{g_t(z) - X_t^{(i)}} + \sqrt{\kappa}\zeta \right) \operatorname{Re} \left(\frac{2X_t^{(j)}}{g_t(w) - X_t^{(j)}} + \sqrt{\kappa}\zeta \right) d \langle M_t^{(i)}, M_t^{(j)} \rangle. \end{aligned}$$

This must coincide with $-dG_{\mathbb{D}}(g_t(z), g_t(w))$, which is similarly computed as in the single-curve case as

$$-dG_{\mathbb{D}}(g_t(z), g_t(w)) = \sum_{i=1}^N \operatorname{Re} \left(\frac{g_t(z) + X_t^{(i)}}{g_t(z) - X_t^{(i)}} \right) \operatorname{Re} \left(\frac{g_t(w) + X_t^{(i)}}{g_t(w) - X_t^{(i)}} \right) dt$$

Therefore, we get $\lambda = 0$ translating to $\chi = \frac{2}{\sqrt{\kappa}} - \frac{\sqrt{\kappa}}{2}$, $\zeta = \frac{1}{\sqrt{\kappa}}$ and $d \langle M_t^{(i)}, M_t^{(j)} \rangle = 0$ for all pairs $i \neq j$.

To conclude, there exist independent standard Brownian motions $(B_t^{(i)} : t \geq 0)$, $i = 1, \dots, N$ and the processes $(\Theta_t^{(i)} : t \geq 0)$, $i = 1, \dots, N$ satisfy the system of SDEs (1.5). The parameters ξ , χ , and ζ are determined in terms of κ as desired. \square

4. HYDRODYNAMIC LIMIT

In the previous section, we saw that coupling between radial multiple SLE and GFF is possible if and only if the radial multiple SLE is driven by the circular Dyson Brownian motions, and concluded that the circular Dyson Brownian motions are the canonical driving processes for radial multiple SLE. This result, along with the fact that the circular Dyson Brownian motions are a stochastic log-gas, motivates us to study the hydrodynamic limit of the radial multiple SLE, the law of large numbers as N tends to infinity.

4.1. Hydrodynamic limit of circular Dyson Brownian motions. We start with the hydrodynamic limit of circular Dyson Brownian motions. Let $\beta > 0$ be fixed. For each

$N \geq 1$, the N -particle circular β -Dyson Brownian motions $(X_t^{(i)} : t \geq 0)$, $i = 1, \dots, N$ give rise to a measure-valued process

$$\Xi_t^{[N]}(\cdot) = \frac{1}{N} \sum_{i=1}^N \delta_{X_{t/N}^{(i)}}(\cdot), \quad t \geq 0.$$

Notice the time-change $t \rightarrow t/N$ on the particles. The following is a consequence of [CL01, Theorem 4.1].

Proposition 4.1. *Assume that $\Xi_0^{[N]}(\cdot)$ converges weakly to $\mu_0(\cdot)$ as $N \rightarrow \infty$. The sequence of measure-valued processes $(\Xi_t^{[N]}(\cdot) : t \geq 0)$, $N \geq 1$ almost surely weakly converges to a unique measure-valued process $(\mu_t(\cdot) : t \geq 0)$ as $N \rightarrow \infty$. Furthermore, the limit process is characterized by its circular Stieltjes transform*

$$(4.1) \quad M_t(z) := \int_{\mathbb{S}} \frac{x+z}{x-z} \mu_t(dx), \quad z \in \mathbb{C} \setminus \text{supp } \mu_t \quad t \geq 0,$$

that solves the partial differential equation

$$(4.2) \quad \frac{\partial M_t(z)}{\partial t} + 2z M_t(z) \frac{\partial M_t(z)}{\partial z} = 0$$

under the initial condition

$$(4.3) \quad M_0(z) = \int_{\mathbb{S}} \frac{x+z}{x-z} \mu_0(dx), \quad z \in \mathbb{C} \setminus \text{supp } \mu_0.$$

We may think of (4.2) as the *complex Burgers equation in the inviscid limit* on the unit circle \mathbb{S} that has its origin in hydrodynamics. This is the reason for us calling the limit process $(\mu_t(\cdot) : t \geq 0)$ the *hydrodynamic limit* of the circular Dyson Brownian motions. Notice that the dependence on the parameter $\beta > 0$ disappears in this limit.

Remark 4.2. To be precise, the limit process in [CL01, Theorem 4.1] is characterized by the Burgers equation with a diffusion term that we do not have in (4.2). This difference arises from the fact that, in [CL01], the Brownian motions scale differently from ours as $N \rightarrow \infty$. However, it is rather straightforward to see in the proof of [CL01, Theorem 4.1] that we may just drop the diffusion term with our scaling of the Brownian motions. Detailed analysis with the same scaling as ours can also be found in [HS21].

Remark 4.3. As we recalled in Remark 3.6, the circular β -Dyson Brownian motions almost surely collide when $0 < \beta < 1$ in their original time scale. Nonetheless, after the time change $t \rightarrow t/N$, the limit process $(\mu_t(\cdot) : t \geq 0)$ can evolve till infinity.

Lemma 4.4. *The solution of (4.2) under the initial condition (4.3) is given by*

$$M_t(z) = M_0(e^{-2tM_t(z)}z), \quad z \in \mathbb{C} \setminus \text{supp } \mu_t, \quad t \geq 0.$$

Proof. We apply the method of characteristics. In our case, we can simply use the time t as the parameter for the characteristic curves. In fact, when we set $z(t) = we^{2tM_0(w)}$, $t \geq 0$ for a fixed w , $M_t(z(t))$ stays constant in t . In particular, we have

$$M_t(z(t)) = M_0(w) = M_0(e^{-2tM_t(z(t))}z(t)), \quad t \geq 0.$$

For each z , we may find w such that $z(t) = z$. Therefore, the above equation gives the desired result. \square

The limit measure μ_t , $t > 0$ has a smooth density $\mu_t(dx) = \rho_t(x)dx$ with respect to the Lebesgue measure dx on \mathbb{S} [CL01, Theorem 6.1]. For the present circular setting, the Sokhotski–Plemelj theorem [AF03, Chapter 7] gives

$$\rho_t(x) = \operatorname{Re} \left\{ \lim_{r \uparrow 1} \frac{1}{2\pi} M_t(rx) \right\} = \operatorname{Re} \left\{ \lim_{r \downarrow 1} \frac{1}{2\pi} M_t(rx) \right\}, \quad x \in \mathbb{S}, \quad t \geq 0.$$

We consider the case (1.6). That is, the hydrodynamic limit of the circular Dyson Brownian motions starts from a single source at $z = 1$,

$$(4.4) \quad \mu_0(\cdot) = \delta_1(\cdot).$$

Then, the initial condition (4.3) is given by

$$(4.5) \quad M_0(z) = \int_{\mathbb{S}} \frac{x+z}{x-z} \delta_1(dx) = \frac{1+z}{1-z}, \quad z \in \mathbb{C} \setminus \{1\}.$$

By Lemma 4.4, the solution $(M_t(z) : t \geq 0)$ of the inviscid complex Burgers equation (4.2) on \mathbb{S} satisfies the functional equation,

$$M_t(z) = \frac{1 + e^{-2tM_t(z)}z}{1 - e^{-2tM_t(z)}z},$$

or equivalently,

$$(4.6) \quad z = e^{2tM_t(z)} \frac{M_t(z) - 1}{M_t(z) + 1}.$$

We assume that $z = re^{i\phi}$, $r > 1$ and take the radial part of (4.6). If we write $M_t(z) = M^R + iM^I$, $M^R, M^I \in \mathbb{R}$, then we have $r = |e^{2t(M^R + iM^I)}(M^R + iM^I - 1)/(M^R + iM^I + 1)|^2$, which gives

$$(4.7) \quad (M^I)^2 = -(M^R)^2 + 2M^R \coth(2tM^R - \log r) - 1.$$

We take the limit $r \downarrow 1$ in (4.7) under a fixed ϕ . If $\rho_t(e^{i\phi}) = 0$, $M^R \rightarrow 0$ under this limit. Thus, in this case, we need more information for M^R to take the limit of (4.7). Otherwise, we just get

$$(4.8) \quad (M^I(\phi))^2 = -(M^R(\phi))^2 + 2M^R(\phi) \coth(2tM^R(\phi)) - 1$$

for ϕ such that $\rho_t(e^{i\phi}) > 0$. Here, we manifested the dependence on ϕ . This means that we can extend $M_t(z)$ to $z = e^{i\phi}$ such that $\rho_t(e^{i\phi}) > 0$.

If $\operatorname{supp} \mu_t$ has any edge $e^{i\phi_t^c}$ on \mathbb{S} , $\phi_t^c \in (-\pi, \pi]$, it is determined by

$$\lim_{\substack{\phi \rightarrow \phi_t^c \\ \rho_t(e^{i\phi}) > 0}} \rho_t(e^{i\phi}) = 0.$$

When we take the corresponding limit $M^R(\phi) \rightarrow 0$ in (4.8), we have $(M^I(\phi))^2 \rightarrow 1/t - 1$. Thus, the edge $e^{i\phi_t^c}$ exists when $t \leq 1$ and M_t is extended to $z = e^{i\phi_t^c}$ as $M_t(e^{i\phi_t^c}) =$

$\pm i\sqrt{1/t-1}$. By putting this back to (4.6), we can determine ϕ_t^c as

$$\begin{aligned} e^{\pm i\phi_t^c} &= e^{\pm 2i\sqrt{t(1-t)}} \left[1 - 2t \pm 2i\sqrt{t(1-t)} \right] \\ &= \exp[\pm i(\arccos(1-2t) + 2\sqrt{t(1-t)})]. \end{aligned}$$

Let us put

$$(4.9) \quad \phi_t^c = \arccos(1-2t) + 2\sqrt{t(1-t)}.$$

We have just confirmed that $\text{supp } \mu_t$ has edges on \mathbb{S} given by $e^{\pm i\phi_t^c}$ in pair as long as $t \leq 1$. It is easy to verify that ϕ_t^c is increasing in $t \in [0, 1]$ with $\phi_0^c = 0$ and $\phi_1^c = \pi$. Hence, we can conclude the following.

Proposition 4.5. *here is a critical time $t_c = 1$ such that*

- (1) *if $0 < t < t_c$, then the support of μ_t is an arc given by*

$$\text{supp } \mu_t = \{e^{i\phi} \mid \phi \in [-\phi_t^c, \phi_t^c]\},$$

- (2) *if $t \geq t_c$, then the support of μ_t extends over \mathbb{S} ; $\text{supp } \mu_t = \mathbb{S}$, where*

- (a) *at $t = t_c$ $\rho_{t_c}(x) > 0$ for $x \in \mathbb{S} \setminus \{-1\}$ and $\rho_{t_c}(-1) = 0$,*
 (b) *at $t \in (t_c, \infty)$, $\rho_t(x) > 0$ for all $x \in \mathbb{S}$.*

4.2. Hydrodynamic limit of multiple SLE and factorization. Associated with the hydrodynamic limit of the circular Dyson Brownian motions, the following limit theorem was proved by Hotta and Schleißinger [HS21]. Let us again fix $\beta > 0$. For $N \in \mathbb{N}$, we write the radial multiple SLE driven by the N -particle circular β -Dyson Brownian motions as $(g_t^{[N]} : t \geq 0)$.

Proposition 4.6 (Hotta and Schleißinger [HS21]). *Under the same assumption as given in Proposition 4.1, as $N \rightarrow \infty$, $g_{t/N}^{[N]}$ converges locally uniformly in distribution to the solution $g_t^{[\infty]}$ of the Loewner chain*

$$(4.10) \quad \frac{d}{dt} g_t^{[\infty]}(z) = g_t^{[\infty]}(z) M_t(g_t^{[\infty]}(z)), \quad t \geq 0,$$

under the initial condition $g_0^{[\infty]}(z) = z \in \mathbb{D}$.

In contrast to (1.4), Equation (4.10) with (4.1) is regarded as a *measure-driven* radial Loewner equation.

The following is the version of [dMS16, Remark 3.11] and [HK18, Lemma 2.1] in the present circular setting. We write $M'_0(y) := \partial M_0(z)/\partial z|_{z=y}$.

Lemma 4.7. *Define a time-dependent map $(h_t : t \geq 0)$ by*

$$h_t(z) = g_t^{[\infty]}(z) e^{-2t M_t(g_t^{[\infty]}(z))}, \quad t > 0,$$

with the initial condition $h_0(z) = g_0^{[\infty]}(z) = z \in \mathbb{D}$. Then the following equality holds,

$$M_t(g_t^{[\infty]}(z)) = M_0(h_t(z)), \quad t \geq 0.$$

Moreover, $h_t(z)$ solves the equation

$$(4.11) \quad \frac{d}{dt}h_t(z) = -\frac{h_t(z)M_0(h_t(z))}{1 + 2th_t(z)M'_0(h_t(z))}, \quad t > 0.$$

Proof. The first equality is an immediate consequence of Lemma 4.4. To derive (4.11), we compute the time derivative of

$$(4.12) \quad g_t^{[\infty]}(z) = h_t(z)e^{2tM_t(g_t^{[\infty]}(z))} = h_t(z)e^{2tM_0(h_t(z))}$$

in two ways. By directly differentiating both sides of (4.12), we get

$$\begin{aligned} \frac{d}{dt}g_t^{[\infty]}(z) &= \frac{d}{dt}h_t(z) \cdot e^{2tM_0(h_t(z))} + h_t(z) \cdot \left(2M_0(h_t(z)) + 2tM'_0(h_t(z)) \frac{d}{dt}h_t(z) \right) e^{2tM_0(h_t(z))} \\ &= (1 + 2th_t(z)M'_0(h_t(z)))e^{2tM_0(h_t(z))} \frac{d}{dt}h_t(z) + 2h_t(z)M_0(h_t(z))e^{2tM_0(h_t(z))}. \end{aligned}$$

This coincides with (4.10) that we can now express as

$$\frac{d}{dt}g_t^{[\infty]}(z) = h_t(z)M_0(h_t(z))e^{2tM_0(h_t(z))}.$$

Comparing the two expressions, we obtain (4.11). \square

Equation (4.12) suggests that the maps $g_t^{[\infty]}$, $t \geq 0$ are naturally factorized into (see Figure 3)

$$(4.13) \quad g_t^{[\infty]} = \Omega_t \circ h_t, \quad t \geq 0$$

with Ω_t defined by the formula

$$\Omega_t(z) := ze^{2tM_0(z)}, \quad t \geq 0.$$

In what follows, we will study the two maps separately to gain knowledge about the Loewner chains $(g_t^{[\infty]} : t \geq 0)$ as well as $(\mathbb{D}_t^{[\infty]} : t \geq 0)$.

Let us define $\tilde{\mathbb{D}}_t := h_t(\mathbb{D}_t)$, $t \geq 0$. Since h_t is univalent on \mathbb{D}_t , it is clear that $h_t : \mathbb{D}_t \rightarrow \tilde{\mathbb{D}}_t$ and $\Omega_t : \tilde{\mathbb{D}}_t \rightarrow \mathbb{D}$ are both conformal maps for each $t \geq 0$. We can also see that the origin 0 is fixed by these maps. Therefore, $\tilde{\mathbb{D}}_t$ is equivalently characterized as the neighbor of the origin that Ω_t conformally maps to \mathbb{D} .

4.3. Solution for the Loewner chain. The goal of this subsection is to provide a proof of Theorem 1.5. From now on, we consider the case (4.4), that is $(\mu_t : t \geq 0)$ starts from a single source at $z = 1$. Since (4.5) gives $M'_0(y) = 2/(1 - y)^2$, (4.11) is written as

$$(4.14) \quad \frac{d}{dt}h_t(z) = -\frac{h_t(z)(1 - h_t(z))^2}{1 + h_t(z)(h_t(z) + 4t - 2)}.$$

Lemma 4.8. *Equation (4.14) is solved under the initial condition $h_0(z) = z \in \mathbb{D}$ as*

$$(4.15) \quad t = \left(\frac{1 - h_t(z)}{1 + h_t(z)} \right)^2 \log \left[\frac{(1 - h_t(z))^2 z}{h_t(z)(1 - z)^2} \right].$$

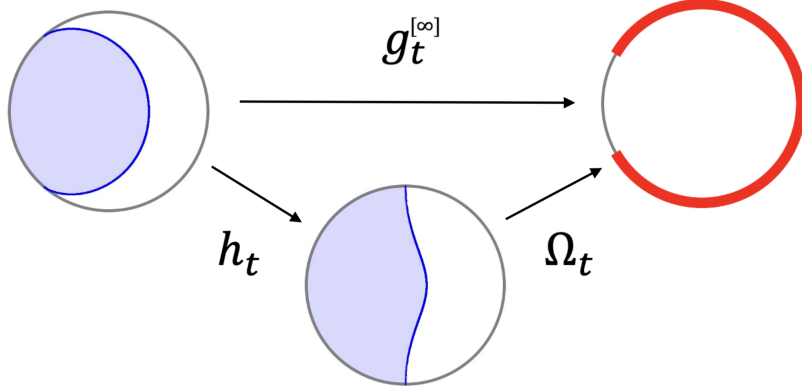


FIGURE 3. In the hydrodynamic limit of the radial multiple SLE, the Loewner chain $g_t^{[\infty]} : \mathbb{D}_t^{[\infty]} \rightarrow \mathbb{D}$, $t \geq 0$ is factorized into two steps, $h_t : \mathbb{D}_t^{[\infty]} \rightarrow \tilde{\mathbb{D}}_t$ and $\Omega_t : \tilde{\mathbb{D}}_t \rightarrow \mathbb{D}$. Figure shows the system at time $t = 0.5 < t_c$ started from δ_1 . The support of the hydrodynamic limit μ_t of the circular Dyson Brownian motion indicated by a red arc in the upper right figure is the image of the boundary curve γ_t by $g_t^{[\infty]}$ as well as that of $\tilde{\gamma}_t$ by Ω_t . In the text, we use the polar coordinates, $R_t e^{i\varphi_t} \in \mathbb{D}_t^{[\infty]}$, $r_t e^{i\theta_t} \in \tilde{\mathbb{D}}_t$, and $s_t e^{i\phi_t} \in \mathbb{D}$, $t \geq 0$, respectively.

Proof. Equation (4.14) is written as

$$(4.16) \quad dt = -\frac{4t}{1 - h_t(z)^2} dh_t(z) - \frac{1 - h_t(z)}{h_t(z)(1 + h_t(z))} dh_t(z).$$

We use the constant variation method. First we notice that the truncated equation

$$dt = -\frac{4t}{1 - h_t(z)^2} dh_t(z) \quad \Longleftrightarrow \quad \frac{dt}{2t} = -\frac{dh_t(z)}{1 - h_t(z)} - \frac{dh_t(z)}{1 + h_t(z)}$$

is solved as

$$(4.17) \quad t = c_1 \left(\frac{1 - h_t(z)}{1 + h_t(z)} \right)^2,$$

where c_1 is a constant. Then we consider the variation of c_1 and assume $c_1 = c_1(h_t(z))$. By (4.16) and (4.17), we have the relation,

$$dc_1 = -\frac{1 + h_t(z)}{h_t(z)(1 - h_t(z))} dh_t(z).$$

It is readily integrated as $c_1 = \log\{c_2(1 - h_t(z))^2/h_t(z)\}$ with a constant c_2 . The initial condition $h_0(z) = z$ determines it as $c_2 = z/(1 - z)^2$. If we put the obtained c_1 into (4.17), then we obtain (4.15). \square

We see that (4.15) is written as

$$(4.18) \quad \begin{aligned} t \left[1 + \frac{4h_t(z)}{(1-h_t(z))^2} \right] &= \log \left[\frac{(1-h_t(z))^2}{h_t(z)} \cdot \frac{z}{(1-z)^2} \right] \\ \iff \Lambda_t(h_t(z))e^{\Lambda_t(h_t(z))} &= \Lambda_t(z)e^{-t}, \end{aligned}$$

where $\Lambda_t(z)$ is defined by (1.7).

Equation (4.18) can be solved by using the complex Lambert function similarly to [HK18]. The Lambert W -function is defined as the inverse function of the mapping $x \mapsto xe^x$, which has two real branches with a branching point at $(-e^{-1}, -1)$ in the real plane $(x, W) \in \mathbb{R}^2$ [CGH⁺96, Veb12]. We take the upper branch $W_0(x)$ defined for $x \in [-e^{-1}, \infty)$;

$$(4.19) \quad W_0(x)e^{W_0(x)} = x,$$

where $W_0(0) = 0$, $W_0(e) = 1$, and $W_0(x) \sim x$ as $x \rightarrow 0$. It admits the series expansion

$$W_0(x) = \sum_{n=1}^{\infty} \frac{(-n)^{n-1}}{n!} x^n,$$

whose radius of convergence is e^{-1} . This allows us to extend it to the complex function $W_0(z)$, $|z| < e^{-1}$. In fact, W_0 is analytically continued to $\mathbb{C} \setminus (-\infty, -e^{-1}]$ (see [CGH⁺96] for detail). Comparing (4.18) with (4.19), we conclude

$$W_0(\Lambda_t(z)e^{-t}) = \Lambda_t(h_t(z)) = 4t \frac{h_t(z)}{(1-h_t(z))^2}.$$

By the initial condition $h_0(z) = z$, this provides

$$(4.20) \quad h_t(z) = 1 + \frac{2t}{W_0(\Lambda_t(z)e^{-t})} \left(1 - \sqrt{1 + W_0(\Lambda_t(z)e^{-t})/t} \right), \quad t \geq 0.$$

As for the map Ω_t , $t \geq 0$, we now have the explicit formula

$$(4.21) \quad \Omega_t(z) = z \exp \left(2t \frac{1+z}{1-z} \right), \quad t \geq 0,$$

under the initial condition (4.4) along with (4.5). Putting (4.20) and (4.21) together by the factorization (4.13), we complete the proof of Theorem 1.5.

4.4. Analysis of the map Ω_t . It remains to prove Theorem 1.7. As a step towards it, we first obtain an analogous result for $\tilde{\mathbb{D}}_t$, $t \geq 0$ through the study of the map Ω_t , $t \geq 0$ given by (4.21). In the polar coordinate, $z = re^{i\theta}$, $r \in [0, 1]$, $\theta \in (-\pi, \pi]$, we have

$$\Omega_t(re^{i\theta}) = s_t(r, \cos \theta) e^{i\phi_t(r, \theta)},$$

where

$$(4.22) \quad s_t(r, a) = r \exp \left[\frac{2t(1-r^2)}{1-2ra+r^2} \right],$$

$$(4.23) \quad \phi_t(r, \theta) = \theta + \frac{4tr \sin \theta}{1-2r \cos \theta + r^2}.$$

We study the condition $\Omega_t(re^{i\theta}) \in \mathbb{S}$, that is, solutions of the equation $s_t(r, \cos \theta) = 1$, in detail. It is obvious that $\Omega_t(0) = 0$, and (4.22) satisfies $s_t(1, a) = 1$ for $a \neq 1$. When $a = 1$, we can readily verify that $s_t(r, 1)$ is increasing in r and $s_t(r, 1) \uparrow \infty$ as $r \uparrow 1$. Otherwise, we have

$$\frac{\partial s_t(r, a)}{\partial r} = U_{t,a}(r)q_{t,a}^+(r)q_{t,a}^-(r)$$

with

$$U_{t,a}(r) = \frac{1}{(1 - 2ra + r^2)^2} \exp \left[\frac{2t(1 - r^2)}{1 - 2ra + a^2} \right],$$

$$q_{t,a}^\pm(r) = r^2 + 2[-a(1 - t) \pm \sqrt{A_{t,a}}]r + 1,$$

where $A_{t,a} = t[2(1 - a^2) + a^2t] \geq 0$ for $t \geq 0$ and $a \in [-1, 1)$. It is obvious that $U_{t,a}(r) > 0$, $0 \leq r < 1$. By straightforward calculation, we can prove the following.

- (1) For $t > 0$ and $a \in [-1, 1)$, $q_t^+(r)$ does not have any root in $(0, 1)$.
- (2) When $0 < t \leq 1$, if $-1 \leq a < 1 - 2t$, $q_t^-(r)$ does not have any root in $(0, 1)$, but if $1 - 2t \leq a < 1$, $q_t^-(r)$ has a unique root $r_{t,a}^* \in (0, 1)$.
- (3) When $t > 1$, $q_t^-(r)$ has a unique root $r_{t,a}^* \in (0, 1)$ for any $a \in [-1, 1)$.

Let $a \in [-1, 1)$ be fixed. Since $s_t(0, a) = 0 < s_t(1, a) = 1$, if there is only one root $r_{t,a}^* \in (0, 1)$, $s_t(r_{t,a}^*, a) > 1$ is a maximal value for $r \in (0, 1)$, and hence $s_t(r, a)$ hits 1 at some $r \in (0, r_{t,a}^*)$. Therefore, the equation $s_t(r, a) = 1$ has one or two solutions in $(0, 1]$, where one of them is the trivial solution $r = 1$, and other solution is in $(0, r_{t,a}^*)$, if exists. For $\theta \in (-\pi, \pi]$, we define $r_t(\theta)$ as the smallest solution of $s_t(r, \cos \theta) = 1$. Obviously, $r_t(\theta) = r_t(2\pi - \theta)$, because $s_t(r, \cos \theta)$ only depends on $\cos \theta$. We can also see that, when $t \leq 1$, there is a critical angle $\theta_t^c \in [0, \pi]$ such that $r_t(\theta) < 1$ for $-\theta_t^c < \theta < \theta_t^c$, and $r_t(\theta) = 1$ for $\theta_t^c \leq \theta \leq \pi$ or $-\pi < \theta \leq -\theta_t^c$, while when $t > 1$, $r_t(\theta) < 1$ for all $\theta \in (-\pi, \pi]$.

At this point, we may identify $\widetilde{\mathbb{D}}_t$, $t > 0$ as

$$\widetilde{\mathbb{D}}_t = \{re^{i\theta} \mid 0 \leq r < r_t(\theta), \theta \in (-\pi, \pi]\},$$

but we would be interested in the part of $\partial\widetilde{\mathbb{D}}_t$ that runs in \mathbb{D} . The key observation is that, if $r_t(\theta) < 1$, the equation $s_t(r_r(\theta), \cos \theta) = 1$ with (4.22) is written as

$$\theta = \arccos F_t(r_t(\theta)),$$

where

$$(4.24) \quad F_t(r) = \frac{t(1 - r^2)}{r \log r} + \frac{1 + r^2}{2r}, \quad 0 < r < 1.$$

Let us set $I_t := F_t^{-1}([-1, 1])$. We can see that $F_t(r)$ is monotonically decreasing in $r \in I_t$ regardless of $t > 0$. When $0 < t \leq 1$, we have $I_t = [r_t^{\min}, 1)$ with $r_t^{\min} \in (0, 1)$ defined as the unique solution of

$$(4.25) \quad F_t(r_t^{\min}) = 1 \quad \Longleftrightarrow \quad t = -\frac{1 - r_t^{\min}}{2(1 + r_t^{\min})} \log r_t^{\min},$$

and

$$\lim_{r \uparrow 1} F_t(r) = 1 - 2t.$$

Therefore, the critical angle is explicitly determined as

$$(4.26) \quad \theta_t^c = \arccos(1 - 2t) \in (0, \pi], \quad t \leq 1.$$

When $t > 1$, we have $I_t = [r_t^{\min}, r_t^{\max}]$, where r_t^{\min} is given by the same formula (4.25) and $r_t^{\max} \in (0, 1)$ is the unique solution of

$$(4.27) \quad F_t(r_t^{\max}) = -1 \quad \Longleftrightarrow \quad t = -\frac{1 + r_t^{\max}}{2(1 - r_t^{\max})} \log r_t^{\max}.$$

With the critical time $t_c = 1$, we define a simple curve in \mathbb{D} by

$$(4.28) \quad \tilde{\gamma}_t = \begin{cases} \{re^{i\theta} \mid \theta = \arccos F_t(r), r \in [r_t^{\min}, 1)\} \cup \{e^{\pm i\theta_t^c}\}, & \text{if } 0 \leq t \leq t_c, \\ \{re^{i\theta} \mid \theta = \arccos F_t(r), r \in [r_t^{\min}, r_t^{\max}]\}, & \text{if } t_c < t < \infty. \end{cases}$$

Note that, unless $r = r_t^{\min}$ or r_t^{\max} , there are two θ 's satisfying the equation for a given r . It is clear that $\tilde{\gamma}_t$ splits \mathbb{D} into two parts. The analogue of Theorem 1.7 for $\tilde{\mathbb{D}}_t$ goes as follows (see Figure 4 for illustration).

Proposition 4.9. *At each $t \geq 0$, $\tilde{\mathbb{D}}_t$ is the connected component of $\mathbb{D} \setminus \tilde{\gamma}_t$ that contains 0.*

Finally, if we set $r = 1$ in (4.23), we get

$$\phi_t(1, \theta) = \theta + \frac{2t \sin \theta}{1 - \cos \theta} = \theta + 2t \cot(\theta/2).$$

Since (4.26) gives $\sin(\theta_t^c/2) = \sqrt{t}$ and $\cos(\theta_t^c/2) = \sqrt{1-t}$, we have

$$\phi_t(1, \theta_t^c) = \arccos(1 - 2t) + 2\sqrt{t(1-t)}, \quad 0 \leq t \leq t_c.$$

This is exactly equal to ϕ_t^c given by (4.9). Then we can conclude the following.

Proposition 4.10. *For $t > 0$, the support of the hydrodynamic limit of the circular Dyson Brownian motions μ_t on \mathbb{S} is the image of the curve $\tilde{\gamma}_t$ in \mathbb{D} by the map Ω_t ;*

$$\text{supp } \mu_t = \Omega_t(\tilde{\gamma}_t), \quad t > 0.$$

4.5. Boundary curve of the SLE hull. Let us finalize the proof of Theorem 1.7. We shall define $\hat{\gamma}_t := h_t^{-1}(\tilde{\gamma}_t)$, $t \geq 0$ and show that it coincides with γ_t , $t \geq 0$ defined in (1.14). Combined with Proposition 4.9, we may conclude Theorem 1.7.

Let us fix $t \geq 0$. The key identity for determining $\hat{\gamma}_t$ is (4.18). In order to exploit it effectively, let us first observe that $\Lambda_t(e^\zeta) = t/\sinh^2(\zeta/2)$. In this new variable, (4.18) gives

$$(4.29) \quad \sinh^2 \frac{\zeta}{2} = \frac{te^{-t}}{\Lambda_t(h_t(e^\zeta))e^{\Lambda_t(h_t(e^\zeta))}}.$$

Let us investigate $\Lambda_t(h_t(e^\zeta))$ for such ζ that $h_t(e^\zeta) \in \tilde{\gamma}_t$ in more detail.

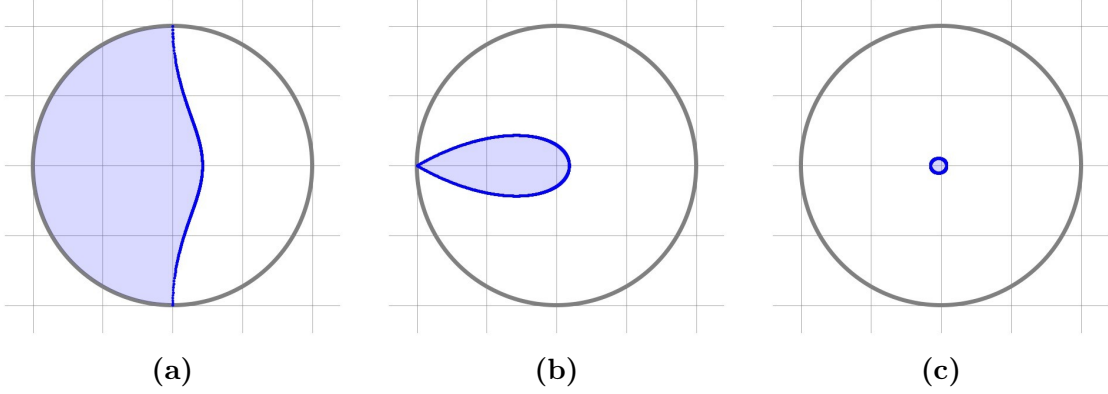


FIGURE 4. The domains \mathbb{D}_t of the map Ω_t are shown by the shaded subdomains of \mathbb{D} and the curves $\tilde{\gamma}_t$ are drawn by tick lines for (a) $t = 0.5$, (b) $t = t_c = 1$ (critical time), (c) $t = 1.5$, respectively.

In the polar coordinates $z = re^{i\theta}$, (1.7) has the following expression:

$$\Lambda_t(re^{i\theta}) = \frac{4tr}{1 - 2r \cos \theta + r^2} e^{i\varpi(r, \cos \theta)}, \quad t \geq 0,$$

with

$$\cos \varpi(r, a) = \frac{(1 + r^2)a - 2r}{1 - 2ra + r^2}.$$

When $re^{i\theta} \in \tilde{\gamma}_t$ with $\theta \in [0, \pi]$, $\Lambda_t(re^{i\theta})$ is a function only of r because θ is uniquely determined by (4.28). Let us set

$$\tilde{\Lambda}_t(r) := \Lambda_t(re^{i\theta}) \Big|_{\theta = \arccos F_t(r) \in [0, \pi]} = \tilde{u}(r) e^{2i\tilde{\psi}_t(r)}$$

with

$$\begin{aligned} \tilde{u}(r) &= \frac{4tr}{1 - 2rF_t(r) + r^2} = -\frac{2r \log r}{1 - r^2}, \\ \cos(2\tilde{\psi}_t(r)) &= \cos \varpi(r, F_t(r)) = -\frac{(1 - r^2) \log r}{4tr} - \frac{1 + r^2}{2r}. \end{aligned}$$

Then, (4.29) allows us to express $\zeta \in \mathbb{C}$ such that $e^\zeta \in \hat{\gamma}_t \cap \overline{\mathbb{H}}$ as

$$\begin{aligned} \zeta &= \tilde{\Phi}_t(r) := 2 \operatorname{arcsinh} \left[-\sqrt{\frac{te^{-t}}{\tilde{\Lambda}_t(r)e^{\tilde{\Lambda}_t(r)}}}} \right] \\ &= 2 \operatorname{arcsinh} \left[-\sqrt{\frac{te^{-t}}{\tilde{u}(r)}} \exp \left(-i\tilde{\psi}_t(r) - \frac{1}{2}\tilde{u}(r)e^{2i\tilde{\psi}_t(r)} \right) \right] \end{aligned}$$

with some allowed r . Notice that the function (1.9) is identified as $\Phi_t(x) = \tilde{\Phi}_t(e^{-x})$. When we set $x_t^{\min} = -\log r_t^{\max}$ and $x_t^{\max} = -\log r_t^{\min}$, the definitions of r_t^{\min} and r_t^{\max} in (4.25) and (4.27) are translated to (1.8). We have just seen that $\hat{\gamma}_t \cap \overline{\mathbb{H}} = \gamma_t^+$, but we can conclude that $\hat{\gamma}_t = \gamma_t$ due to the reflection symmetry against the real axis.

4.6. Edge asymptotics. As long as $t \leq t_c = 1$, the boundary curve γ_t hits the unit circle at $e^{\pm i\varphi_t^c}$ with the critical angle φ_t^c given in (1.13). Let us take a closer look at the behaviour of γ_t in the vicinity of the edges. We define $R_t(\varphi) \in (0, 1]$, $\varphi \in [-\varphi_t^c, \varphi_t^c]$ by $\gamma_t = \{R_t(\varphi)e^{i\varphi} | \varphi \in [-\varphi_t^c, \varphi_t^c]\}$.

Proposition 4.11. (1) For $0 < t < t_c$, $R_t(\varphi)$ behaves in the vicinity of φ_t^c as

$$(4.30) \quad 1 - R_t(\varphi) \sim b_t(\varphi_t^c - \varphi)^\nu \quad \text{as } \varphi \uparrow \varphi_t^c \quad \text{with } \nu = \frac{3}{2},$$

where the coefficient

$$b_t = \frac{\sqrt{2}}{3t^{1/4}(1-t)} \left(\frac{1-te^{1-t}}{e^{1-t}} \right)^{1/4}$$

diverges as

$$b_t \sim \frac{\sqrt{2}}{3}(1-t)^{-\sigma} \uparrow +\infty \quad \text{as } t \uparrow t_c \quad \text{with } \sigma = \frac{3}{4}.$$

(2) At $t = t_c$, we have

$$(4.31) \quad 1 - R_{t_c}(\varphi) \sim \frac{1}{\sqrt{3}}(\varphi_{t_c}^c - \varphi) \quad \text{as } \varphi \uparrow \varphi_{t_c}^c = \pi.$$

Proof. For $0 < x \ll 1$, (1.10) gives

$$u(x) = 1 - \frac{x^2}{6} + \frac{7x^4}{360} + \mathcal{O}(x^6).$$

(1) If $0 < t < t_c$, (1.11) gives

$$\psi_t(x) = \frac{\pi}{2} - \frac{1}{2} \left(\frac{1-t}{t} \right)^{1/2} x - \frac{1}{48t^{3/2}(1-t)^{1/2}} x^3 + \mathcal{O}(x^5),$$

and then (1.9) is written as

$$\Phi_t(x) = 2\text{arcsinh} \left[it^{1/2}e^{(1-t)/2} - c_t^R x^3 - ic_t^I x^2 + \mathcal{O}(x^4) \right],$$

where

$$c_t^R = \frac{(1-t)^{1/2}}{12t} e^{(1-t)/2}, \quad c_t^I = \frac{t^{1/2}(1-t)}{4t} e^{(1-t)/2}.$$

For the moment, let us put $R_t(x)e^{i\varphi_t(x)} := e^{\Phi_t(x)}$ so that both $R_t(x)$ and $\varphi_t(x)$ are regarded as functions of x . Then, (1.12) with (1.9) gives

$$\begin{aligned} & it^{1/2}e^{(1-t)/2} - c_t^R x^3 - ic_t^I x^2 + \mathcal{O}(x^4) \\ &= i \sin(\varphi_t^c/2) - \frac{1}{2}(1 - R_t(x)) \cos(\varphi_t^c/2) - i \frac{1}{2}(\varphi_t^c - \varphi_t(x)) \cos(\varphi_t^c/2). \end{aligned}$$

Since we have $\sin(\varphi_t^c/2) = t^{1/2}e^{(1-t)/2}$ from (1.13), we get

$$1 - R_t(x) \sim \frac{2c_t^R}{\cos(\varphi_t^c/2)} x^3, \quad \varphi_t^c - \varphi_t(x) \sim \frac{2c_t^I}{\cos(\varphi_t^c/2)} x^2$$

by comparing the real and imaginary parts. The assertion (1) follows because $\varphi_t(x) \uparrow \varphi_t^c$ as $x \downarrow 0$.

(2) If $t = t_c$, (1.11) gives

$$\psi_{t_c}(x) = \frac{\pi}{2} - \frac{x^2}{4\sqrt{3}} - \frac{x^4}{120\sqrt{3}} + \mathcal{O}(x^6),$$

and then (1.9) is written as

$$\Phi_{t_c}(x) = 2\operatorname{arcsinh} \left[\mathbf{i} - \frac{1}{72}(\sqrt{3} + \mathbf{i})x^4 + \mathcal{O}(x^6) \right].$$

Therefore, we can verify that $1 - R_{t_c}(x) \sim x^2/(3\sqrt{2})$, $\varphi_{t_c}^c - \varphi_{t_c}(x) \sim x^2/\sqrt{6}$, and hence (4.31) is proved. \square

Similar asymptotic analysis is possible for the edges of $\tilde{\gamma}_t$ with $0 < t \leq t_c$. In fact, (4.24) admits the expansion

$$F_t(r) = 1 - 2t + \frac{1}{6}(3 - 2t)(1 - r)^2 + \mathcal{O}((1 - r)^3) \quad \text{as } r \uparrow 1.$$

Note that the curve $\tilde{\gamma}_t$ can be parametrized as $\tilde{\gamma}_t = \{r_t(\theta)e^{\mathbf{i}\theta} | \theta \in [-\theta_t^c, \theta_t^c]\}$. We can verify the following.

Proposition 4.12. *The curve $\tilde{\gamma}_t$, $0 < t \leq t_c$ behaves as follows in the vicinity of the edge $e^{\mathbf{i}\theta_t^c}$.*

(1) For $0 < t < t_c$,

$$1 - r_t(\theta) \sim a_t(\theta_t^c - \theta)^{\nu'} \quad \text{as } \theta \uparrow \theta_t^c \quad \text{with } \nu' = \frac{1}{2},$$

where the coefficient

$$a_t = \frac{2(t(1 - t))^{1/4}}{(1 - 2t/3)^{1/2}}.$$

vanishes as

$$a_t \sim 2\sqrt{3}(1 - t)^{\sigma'} \downarrow 0 \quad \text{as } t \uparrow t_c \quad \text{with } \sigma' = \frac{1}{4}.$$

(2) At $t = t_c$,

$$1 - r_{t_c}(\theta) \sim \sqrt{3}(\theta_{t_c}^c - \theta) \quad \text{as } \theta \uparrow \theta_{t_c}^c = \pi.$$

By comparing (1.13) and (4.26), we always have $\varphi_t^c > \theta_t^c$ for $0 < t < t_c$. This accompanies the fact that $\nu' = 1/2 < 3/2 = \nu$. In fact, it can be visually seen that the edge behavior of γ_t (Figure 2 (a)) is sharper than that of $\tilde{\gamma}_t$ (Figure 4 (a)).

We recall that the edge exponent $\nu = 3/2$ for $0 < t < t_c$ in (4.30) is the same value with the edge exponent obtained by [HK18] in the chordal setting. In this sense, we could say that ν is a *universal* exponent.

As t approaches t_c , the coefficient b_t in the edge asymptotics for γ_t (*susceptibility*, let us call it) diverges and the exponent eventually turns to unity at $t = t_c$. For $\tilde{\gamma}_t$, the opposite is observed; the coefficient a_t vanishes, but the exponent at $t = t_c$ is again unity.

Because of these characteristics, we would like to regard the singularity at $t = t_c$ as a *critical phenomenon*.

Let us close this section by stressing a few aspects that we think are significant. First, the critical phenomenon is a new feature of the radial setting; there is no analogue in the chordal setting [HK18]. Second, the critical phenomenon can only be observed in the hydrodynamic limit $N \rightarrow \infty$. This is natural since a critical phenomenon occurs in an infinite system. Lastly, even though a singularity at $t = t_c$ is already observed for the hydrodynamic limit of circular Dyson Brownian motions when $\text{supp}\mu_t$ changes its topology, the critical phenomenon only occurs at the level of multiple SLE. With that, we say that the singularity for $\text{supp}\mu_t$ is a shadow of a critical phenomenon.

REFERENCES

- [AB24] J. Aru and P. Bordenave. SLE and its partition function in multiply connected domains via the Gaussian Free Field and restriction measures. *arXiv:2405.20148*, 2024.
- [ABG12] R. Allez, J.-P. Bouchaud, and A. Guionnet. Invariant beta ensembles and the Gauss-Wigner crossover. *Phys. Rev. Lett.*, 109(9):094102, 2012.
- [ABK24] T. Alberts, S.-S. Byun, and N.-G. Kang. Conformal field theory of Gaussian free fields in a multiply connected domain. *arXiv:2407.08220*, 2024.
- [ACSW24] M. Ang, G. Cai, X. Sun, and B. Wu. SLE loop measure and Liouville quantum gravity. *arXiv:2409.16547*, 2024.
- [AF03] M. J. Ablowitz and A. S. Fokas. *Complex variables: introduction and applications*. Cambridge University Press, 2003.
- [AG13] R. Allez and A. Guionnet. A diffusive matrix model for invariant β -ensembles. *Electron. J. Probab.*, 18:1–30, 2013.
- [AGZ10] G. W. Anderson, A. Guionnet, and O. Zeitouni. *An Introduction to Random Matrices*. Cambridge University Press, Cambridge, 2010.
- [AHP24] O. Abuzaid, V. O. Healey, and E. Peltola. Large deviations of Dyson Brownian motion on the circle and multiradial SLE $_{0+}$. *arXiv:2407.13762*, 2024.
- [AHS23a] M. Ang, N. Holden, and X. Sun. Conformal welding of quantum disks. *Electron. J. Probab.*, 28:1–50, 2023. DOI: 10.1214/23-EJP943.
- [AHS23b] M. Ang, N. Holden, and X. Sun. The SLE loop via conformal welding of quantum disks. *Electron. J. Probab.*, 28:1–20, 2023. DOI: 10.1214/23-EJP914, arXiv:2205.05074.
- [AHS24] M. Ang, N. Holden, and X. Sun. Integrability of SLE via conformal welding of random surfaces. *Commun. Pure and Appl. Math.*, 77(5):2651–2707, 2024.
- [AHSY23] M. Ang, N. Holden, X. Sun, and P. Yu. Conformal welding of quantum disks and multiple SLE: the non-simple case. *arXiv:2310.20583*, 2023.
- [BB02] M. Bauer and D. Bernard. SLE $_{\kappa}$ growth processes and conformal field theories. *Phys. Lett. B*, 543:135–138, 2002.
- [BB03] M. Bauer and D. Bernard. Conformal field theories of stochastic Loewner evolutions. *Commun. Math. Phys.*, 239:493–521, 2003.
- [BB04a] M. Bauer and D. Bernard. CFTs of SLEs: the radial case. *Phys. Lett. B*, 583:324–330, 2004.
- [BB04b] M. Bauer and D. Bernard. Conformal transformations and the SLE partition function martingale. *Ann. Henri Poincaré*, 5:289–326, 2004.
- [BBK05] M. Bauer, D. Bernard, and K. Kytölä. Multiple Schramm–Loewner evolutions and statistical mechanics martingales. *J. Stat. Phys.*, 120:1125–1163, 2005.
- [BF06] R. O. Bauer and R. M. Friedrich. On radial stochastic Loewner evolution in multiply connected domains. *J. Funct. Anal.*, 237(2):565–588, 2006.

- [BF08] R. Bauer and R. Friedrich. On chordal and bilateral SLE in multiply connected domains. *Math. Z.*, 258:241–265, 2008.
- [BKT23] S.-S. Byun, N.-G. Kang, and H.-J. Tak. Conformal field theory for annulus SLE: partition functions and martingale-observables. *Analysis and Mathematical Physics*, 13(1):1, 2023.
- [BP25] N. Berestycki and E. Powell. *Gaussian free field and Liouville quantum gravity*. Cambridge University Press, 2025. arXiv:2404.16642.
- [BPW21] V. Beffara, E. Peltola, and H. Wu. On the uniqueness of global multiple SLEs. *Ann. Probab.*, 49:400–434, 2021.
- [BPZ84a] A. A. Belavin, A. M. Polyakov, and A. B. Zamolodchikov. Infinite conformal symmetry in two-dimensional quantum field theory. *Nucl. Phys. B*, 241:333–380, 1984.
- [BPZ84b] A. A. Belavin, A. M. Polyakov, and A. B. Zamolodchikov. Infinite conformal symmetry of critical fluctuations in two dimensions. *J. Stat. Phys.*, 34:763–774, 1984.
- [Car03] J. Cardy. Stochastic Loewner evolution and Dyson’s circular ensembles. *J. Phys. A: Math. Gen.*, 36:L379–L386, 2003. Corrigendum, *ibid.* 12343.
- [CDCH⁺14] D. Chelkak, H. Duminil-Copin, C. Hongler, A. Kemppainen, and S. Smirnov. Convergence of Ising interfaces to Schramm’s SLE curves. *Comptes Rendus Mathématique*, 352:157–161, 2014.
- [CF18] Z.-Q. Chen and M. Fukushima. Stochastic Komatu–Loewner evolutions and BMD domain constant. *Stochastic Process. Appl.*, 128:545–594, 2018.
- [CFS17] Z.-Q. Chen, M. Fukushima, and H. Suzuki. Stochastic Komatu–Loewner evolutions and SLEs. *Stochastic Process. Appl.*, 127(6):2068–2087, 2017.
- [CGH⁺96] R. M. Corless, G. H. Gonnet, D. E. G. Hare, D. J. Jeffrey, and D. E. Knuth. On the Lambert W function. *Advances in Computational mathematics*, 5:329–359, 1996.
- [CL97] E. Cépa and D. Lépine. Diffusing particles with electrostatic repulsion. *Probab. Theory Relat. Fields*, 107:429–449, 1997.
- [CL01] E. Cépa and D. Lépine. Brownian particles with electrostatic repulsion on the circle: Dyson’s model for unitary random matrices revisited. *ESAIM: Probability and Statistics*, 5:203–224, 2001.
- [CLM23] A. Campbell, K. Luh, and V. Margarint. Rate of convergence in multiple SLE using random matrix theory. *arXiv:2301.04722*, 2023.
- [DE02] I. Dumitriu and A. Edelman. Matrix models for beta ensembles. *J. Math. Phys.*, 43:5830–5847, 2002.
- [DK93] M. R. Douglas and V. A. Kazakov. Large N phase transition in continuum QCD₂. *Phys. Lett. B*, 319(1-3):219–230, 1993.
- [dMHS18] A. del Monaco, I. Hotta, and S. Schleissinger. Tightness results for infinite-slit limits of the chordal Loewner equation. *Comput. Methods Funct. Theory*, 18:9–33, 2018.
- [DMS14] B. Duplantier, J. Miller, and S. Sheffield. Liouville quantum gravity as a mating of trees, 2014. arXiv:1409.7055.
- [dMS16] A. del Monaco and S. Schleissinger. Multiple SLE and the complex Burgers equation. *Math. Nachr.*, 289:2007–2018, 2016.
- [Dre11] S. Drenning. *Excursion reflected Brownian motion and Loewner equations in multiply connected domains*. The University of Chicago, 2011.
- [Dub07] J. Dubédat. Commutation relations for Schramm–Loewner evolutions. *Commun. Pure and Appl. Math.*, LX:1792–1847, 2007.
- [Dub09] J. Dubédat. SLE and the free field: Partition functions and couplings. *J. Amer. Math. Soc.*, 22:995–1054, 2009.
- [Dub15a] J. Dubédat. SLE and Virasoro representations: Fusion. *Commun. Math. Phys.*, 336:761–809, 2015.
- [Dub15b] J. Dubédat. SLE and Virasoro representations: Localization. *Commun. Math. Phys.*, 336:695–760, 2015.

- [Dys62] F. J. Dyson. A Brownian-motion model for the eigenvalues of a random matrix. *J. Math. Phys.*, 3:1191–1198, 1962.
- [FK04] R. Friedrich and J. Kalkkinen. On conformal field theory and stochastic Loewner evolution. *Nucl. Phys. B*, 687:279–302, 2004.
- [FMS11] P. J. Forrester, S. N. Majumdar, and G. Schehr. Non-intersecting Brownian walkers and Yang–Mills theory on the sphere. *Nucl. Phys. B*, 844(3):500–526, 2011.
- [FW03] R. Friedrich and W. Werner. Conformal restriction, highest-weight representations and SLE. *Commun. Math. Phys.*, 243:105–122, 2003.
- [GH23] A. Guionnet and J. Huang. Asymptotics of rectangular spherical integrals. *J. Funct. Anal.*, 285(11):110144, 2023. arXiv preprint arXiv:2106.07146.
- [Gra07] K. Graham. On multiple Schramm–Loewner evolutions. *J. Stat. Mech.*, 2007:P03008, 2007.
- [GW80] D. J. Gross and E. Witten. Possible third-order phase transition in the large- N lattice gauge theory. *Phys. Rev. D*, 21(2):446, 1980.
- [GZ02] A. Guionnet and O. Zeitouni. Large deviations asymptotics for spherical integrals. *J. Funct. Anal.*, 188(2):461–515, 2002.
- [HIM23] C.-P. Huang, D. Inauen, and G. Menon. Motion by mean curvature and Dyson Brownian Motion. *Electron. Commun. Probab.*, 28:1–10, 2023.
- [HK18] I. Hotta and M. Katori. Hydrodynamic limit of multiple SLE. *J. Stat. Phys.*, 171:166–188, 2018.
- [HL21] V. O. Healey and G. F. Lawler. N -sided radial Schramm–Loewner evolution. *Probab. Theory Relat. Fields*, 181(1):451–488, 2021.
- [HP17] D. Holcomb and E. Paquette. Tridiagonal models for Dyson Brownian motion. *arXiv:1707.02700*, 2017.
- [HS21] I. Hotta and S. Schleißinger. Limits of radial multiple SLE and a Burgers–Loewner differential equation. *J. Theor. Probab.*, 34(2):755–783, 2021.
- [IK13] K. Izyurov and K. Kytölä. Hadamard’s formula and couplings of SLEs with free field. *Probab. Theory Relat. Fields*, 155:35–69, 2013.
- [Izy15] K. Izyurov. Smirnov’s observable for free boundary conditions, interfaces and crossing probabilities. *Commun. Math. Phys.*, 337(1):225–252, 2015.
- [Izy17] K. Izyurov. Critical Ising interfaces in multiply-connected domains. *Probab. Theory Relat. Fields*, 167:379–415, 2017.
- [Izy22] K. Izyurov. On multiple SLE for the FK–Ising model. *Ann. Probab.*, 50(2):771–790, 2022.
- [Kar19] A. Karrila. Multiple SLE type scaling limits: from local to global, 2019. arXiv:1903.10354.
- [Kar20] A. Karrila. UST branches, martingales, and multiple SLE(2). *Electron. J. Probab.*, 25:1–37, 2020.
- [Kat15] M. Katori. *Bessel Processes, Schramm–Loewner Evolution, and the Dyson Model*, volume 11 of *SpringerBriefs in Mathematical Physics*. Springer, 2015.
- [Kem17] A. Kemppainen. *Schramm–Loewner Evolution*, volume 24 of *SpringerBriefs in Mathematical Physics*. Springer, 2017.
- [KK20] M. Katori and K. Koshida. Conformal welding problem, flow line problem, and multiple Schramm–Loewner evolution. *J. Math. Phys.*, 61:083301, 2020.
- [KK21a] M. Katori and S. Koshida. Gaussian free fields coupled with multiple SLEs driven by stochastic log-gases. In *Stochastic Analysis, Random Fields and Integrable Probability—Fukuoka 2019*, volume 87, pages 315–341. Mathematical Society of Japan, 2021.
- [KK21b] M. Katori and S. Koshida. Three phases of multiple SLE driven by non-colliding Dyson’s Brownian motions. *J. Phys. A*, 54(32):325002, 2021.
- [KL07] M. Kozdron and G. Lawler. The configuration measure on mutually avoiding SLE paths. In *Universality and Renormalization, Volume 50 of Fields Institute Communications*, pages 199–224. American Mathematical Society, Providence, 2007.
- [KM13] N.-G. Kang and N. G. Makarov. *Gaussian Free Field and Conformal Field Theory*. Astérisque. American Mathematical Society, 2013.

- [Kos21] S. Koshida. Multiple backward Schramm–Loewner evolution and coupling with Gaussian free field. *Lett. Math. Phys.*, 111:30, 2021.
- [KS07] M. Kontsevich and Y. Suhov. On Malliavin measures, SLE, and CFT. *Proceedings of the Steklov Institute of Mathematics*, 258:100–146, 2007.
- [Kyt07] K. Kytölä. Virasoro module structure of local martingales of SLE variants. *Rev. Math. Phys.*, 5:455–509, 2007.
- [Law05] G. F. Lawler. *Conformally Invariant Processes in the Plane*. Amer. Math. Soc., Providence, RI, 2005.
- [Law06] G. F. Lawler. The Laplacian- b random walk and the Schramm–Loewner evolution. *Illinois J. Math.*, 50(1-4):701–746, 2006.
- [Liu25] M. Liu. Critical Ising model, multiple $\text{SLE}_\kappa(\frac{\kappa-6}{2}, \frac{\kappa-6}{2})$ and β -Jacobi ensemble, 2025. arXiv:2504.14595.
- [LSW04] G. F. Lawler, O. Schramm, and W. Werner. Conformal invariance of planar loop-erased random walks and uniform spanning trees. *Ann. Probab.*, 32:939–995, 2004.
- [LW16] K. Liechty and D. Wang. Nonintersecting Brownian motions on the unit circle. *Ann. Probab.*, 44:1134–1211, 2016.
- [MS14] S. N. Majumdar and G. Schehr. Top eigenvalue of a random matrix: large deviations and third order phase transition. *J. Stat. Mech.*, 2014(1):P01012, 2014.
- [MS16a] J. Miller and S. Sheffield. Imaginary geometry I: interacting SLEs. *Probab. Theory Relat. Fields*, 164:553–705, 2016.
- [MS16b] J. Miller and S. Sheffield. Imaginary geometry II: reversibility of $\text{SLE}_\kappa(\rho_1, \rho_2)$ for $\kappa \in (0, 4)$. *Ann. Probab.*, 44:1647–1722, 2016.
- [MS16c] J. Miller and S. Sheffield. Imaginary geometry III: reversibility of SLE_κ for $\kappa \in (4, 8)$. *Ann. Math.*, 184:455–486, 2016.
- [MS17] J. Miller and S. Sheffield. Imaginary geometry IV: interior rays, whole-plane reversibility, and space-filling trees. *Probab. Theory Relat. Fields*, 169:729–869, 2017.
- [Mur19] T. Murayama. Chordal Komatu–Loewner equation for a family of continuously growing hulls. *Stochastic Process. Appl.*, 129(8):2968–2990, 2019.
- [PW19] E. Peltola and H. Wu. Global and local multiple SLE for $\kappa \leq 4$ and connection probabilities for level line of GFF. *Commun. Math. Phys.*, 366:469–536, 2019.
- [PW23a] E. Peltola and Y. Wang. Large deviations of multichordal SLE_{0+} , real rational functions, and zeta-regularized determinants of Laplacians. *Journal of the European Mathematical Society*, 26(2):469–535, 2023.
- [PW23b] E. Peltola and H. Wu. Crossing probabilities of multiple Ising interfaces. *Ann. Appl. Probab.*, 33(4):3169–3206, 2023.
- [RS05] S. Rohde and O. Schramm. Basic properties of SLE. *Ann. Math.*, 161:883–924, 2005.
- [RS17] O. Roth and S. Schleissinger. The Schramm–Loewner equation for multiple slits. *J. Anal. Math.*, 131:73–99, 2017.
- [Sch00] O. Schramm. Scaling limits of loop-erased random walks and uniform spanning trees. *Israel J. Math.*, 118:221–288, 2000.
- [Sch12] S. Schleissinger. The multiple-slit version of Loewner’s differential equation and pointwise Hölder continuity of driving functions. *Ann. Acad. sci. Fenn., Math.*, 37:191–201, 2012. Erratum 49:333–335, 2024.
- [She07] S. Sheffield. Gaussian free fields for mathematicians. *Probab. Theory Relat. Fields*, 139:521–541, 2007.
- [She16] S. Sheffield. Conformal weldings of random surfaces: SLE and the quantum gravity zipper. *Ann. Probab.*, 44:3474–3545, 2016.
- [Smi01] S. Smirnov. Critical percolation in the plane: conformal invariance, Cardy’s formula, scaling limits. *C. R. Acad. Sci. Paris*, 333:239–244, 2001.
- [SS05] O. Schramm and S. Sheffield. Harmonic explorer and its convergence to SLE_4 . *Ann. Probab.*, 33:2127–2148, 2005.

- [SS09] O. Schramm and S. Sheffield. Contour lines of the two-dimensional discrete Gaussian free field. *Acta Math.*, 202:21–137, 2009.
- [SS13] O. Schramm and S. Sheffield. A contour line of the continuum Gaussian free field. *Probab. Theory Relat. Fields*, 157:47–80, 2013.
- [TW94] C. A. Tracy and H. Widom. Level-spacing distributions and the Airy kernel. *Commun. Math. Phys.*, 159(1):151–174, 1994.
- [Veb12] D. Veberič. Lambert W function for applications in physics. *Computer Physics Communications*, 183(12):2622–2628, 2012. arXiv:cs.MS/1209.0735.
- [Wad80] S. R. Wadia. $N = \infty$ phase transition in a class of exactly soluble model lattice gauge theories. *Phys. Lett. B*, 93(4):403–410, 1980.
- [WP22] W. Werner and E. Powell. *Lecture notes on the Gaussian free field*, volume 28 of *Cours Spécialisés*. Société Mathématique de France, 2022. arXiv:2004.04720.
- [Yab23] S. Yabuoku. Eigenvalue processes of symmetric tridiagonal matrix-valued processes associated with Gaussian beta ensemble. *Stochastic Process. Appl.*, 164:139–159, 2023.
- [Zha04] D. Zhan. Stochastic Loewner evolution in doubly connected domains. *Probab. Theory Relat. Fields*, 129:340–380, 2004.

DEPARTMENT OF PHYSICS, FACULTY OF SCIENCE AND ENGINEERING, CHUO UNIVERSITY, KASUGA, BUNKYO-KU, TOKYO 112-8551, JAPAN

Email address: makoto.katori.mathphys@gmail.com

DEPARTMENT OF MATHEMATICS AND SYSTEMS ANALYSIS, AALTO UNIVERSITY, ESPOO, FINLAND

Email address: shinji.koshida@aalto.fi

DEPARTMENT OF PHYSICS, FACULTY OF SCIENCE AND ENGINEERING, CHUO UNIVERSITY, KASUGA, BUNKYO-KU, TOKYO 112-8551, JAPAN

Email address: a22.55ak@g.chuo-u.ac.jp

DEPARTMENT OF PHYSICS, FACULTY OF SCIENCE AND ENGINEERING, CHUO UNIVERSITY, KASUGA, BUNKYO-KU, TOKYO 112-8551, JAPAN

Email address: a22.sjce@g.chuo-u.ac.jp